Acta Astronautica 121 (2016) 200–220

Contents lists available at ScienceDirect

Acta Astronautica

journal homepage: www.elsevier.com/locate/actaastro

Invited Paper

The Highland Terrain Hopper (HOPTER): Concept and use cases of a new locomotion system for the exploration of low gravity Solar System bodies

Daniel Mège [a,b,c,*], Joanna Gurgurewicz [a,d], Jerzy Grygorczuk [a,e], Łukasz Wiśniewski [a,e], Greger Thornell [f]

[a] Space Research Centre, Polish Academy of Sciences, Bartycka St. 18A, 00-716 Warsaw, Poland
[b] Laboratoire de Planétologie et Géodynamique, CNRS UMR 6112, Université de Nantes, BP 92208, 44322 Nantes cedex 3, France
[c] Observatoire des Sciences de l'Univers Nantes Atlantique (OSUNA, CNRS UMS 3281), France
[d] Institute of Geological Sciences, Polish Academy of Sciences, Research Centre in Wrocław, Podwale St. 75, 50-449 Wrocław, Poland
[e] Astronika Sp. z o.o., Bartycka St. 18, 00-716 Warsaw, Poland
[f] Ångström Space Technology Centre, Department of Engineering Sciences, Uppsala University, Box 534, SE-75121 Uppsala, Sweden

ARTICLE INFO

Article history:
Received 11 July 2015
Received in revised form
21 October 2015
Accepted 25 December 2015
Available online 1 January 2016

Keywords:
Planetary locomotion
Planetary geology
Geophysical surveying
Mars
Valles Marineris
Moon

ABSTRACT

Comprehensive understanding of the principles governing the geological activity of the Earth was obtained in continental and oceanic mountains. It is not expected that the principles governing the overall geologic activity and evolution of other planetary bodies such as Mars will be understood if exploration is limited to nearly flat terrains, either imposed by the used exploration platform capabilities, the risk of getting stuck, or by the time required to cross the border of a landing ellipse. Surface exploration of mountains is additionally to be coupled to two- or three-dimensional geophysical surveys to correlate the surface observations with deeper processes. On the small bodies where ultra-low gravity prevails, the weight of wheel-driven platforms is not sufficient to generate the friction at the contact with the ground that is required to trigger motion of the rover relative to the ground. Under such circumstances, hopping is one of the mobility solutions. We present a new locomotion system, the hopter platform, which is adapted to these challenges on Solar System bodies having a gravity field lower than on Earth. The hopter is a robust, versatile and highly manoeuvrable platform based on simple mechanical concepts that accurately jumps to distances of metres to tens of metres and more, depending on the gravity field of the studied body. Its low mass of 10 kg (including up to 3 kg of miniaturised payload), makes it possible to simultaneously launch several hopters to work as a fractionated explorer at a very competitive cost. After reviewing the payload that may be placed onboard hopters, we illustrate the scientific capabilities of hopters and hopter networks in performing basic geologic observations at distinct study sites in a variety of geological environments, obtaining data along steep geological cross sections, surveying geophysical anomalies in the subsurface, prospecting resources, monitoring micro-environments, meteorological events, and geodetic deformation, or characterizing dust activity on Mars, the Moon, and Phobos.

* Corresponding author at: Space Research Centre, Polish Academy of Sciences, Bartycka St. 18A, 00-716 Warsaw, Poland.

http://dx.doi.org/10.1016/j.actaastro.2015.12.042
0094-5765/

1. Introduction

The platforms currently used for the exploration of the solid Solar System bodies include landers and rovers. Immobile lander platforms are powerful for analysis of the ground and environment; their strength is therefore, on the one hand, accurate in situ observations and measurements, such as heat flow measurements [1,2] and determination of thermal and mechanical properties of the subsurface [3], and on the other hand, the ability to monitor events at that site, for instance weather patterns [4,5] and seismic activity [2]. The strength of rovers lies in the possibility of exploring many kilometres on the ground; however two severe restrictions apply: (1) related to landing and trafficability: both place dramatic constraints on slopes and terrain roughness throughout the 10 s of km wide landing ellipse (e.g., [6] for Mars Science Laboratory); (2) related to the surface gravity: roving relies on adherence of wheels to the ground, so that on ultra-low gravity bodies such as Phobos and Deimos, asteroids, cometary nuclei or Kuiper Belt Objects (KBOs), roving is simply not possible.

The landing and trafficability issues cause major problems for geology [7]. Most of the understanding of the Earth gained by field geologists is learnt from mountainous terrain indeed, whether on land or in the sea, because mountains give a three-dimensional view of the geological processes. Roaming around provides information on their geographic extent as well as on their evolution through time (Fig. 1). The terrestrial experience indicates that we cannot save on access and mobility in planetary mountains to gain a sound understanding of the explored body. However, escaping the landing ellipse takes a lot of time; although the dimensions of the landing ellipse for the Mars Science Laboratory Curiosity rover was the smallest ever (7 × 20 km), it took the rover 672 Earth days to cross its landing ellipse border [8], meaning that (1) due to the nearly flat terrain constraints on planetary landing and roving, the view that rovers give us can be compared to the view that geologists would have of the Earth if only kilometres of regions such as the Sahara or the Mississippi delta were explored; (2) the instruments and the main system are already two years old once the 'Sahara reg landing constraints' are released; the observed damages on the MSL wheels testifies to this concern. As an illustration, the lifetime estimate of the MSL wheels on the terrains it has investigated until 2014 corresponds to a travelling distance of 8–14 km, which motivated revision of the planned route to Mount Sharp, its destination [9]. The question of accessing interesting terrains beyond the landing ellipse has been recognised critical [10]. In addition to the landing ellipse constraints, rover wheel slip hazard is critical because slip may break arms or instruments [11]. Slip hazards are many and cause complex challenges, they include low cohesion regolith, moving rocks, small scale slope failures and others. These hazards are aggravated by slope steepness; for instance, MSL has been designed to climb local slopes up to 30° [6], but experience shows that the perspective of a rover tilt by more than 15° requires a specific slip risk assessment procedure to be defined [11].

The wheel adherence issue of rovers is critical on Mars because of the risk of getting stuck if adherence is not high enough; this issue is currently limiting the exploration of ultra-low gravity objects (e.g., asteroids) to landers, i.e. to a study of a single site at the surface, chosen as a function of the landing constraints (slopes, rock abundance, spacecraft motion relative to the studied object etc.) and instrument and overall feasibility requirements (communication with the orbiting spacecraft or the Earth, sunlight etc.). The intrinsic scientific interest of the landing site compared to other potential sites is taken into account in so far as these requirements are satisfied. Landing of Philae on comet 67P/Churyumov-Gerasimenko is an example of this approach [12]; although the lander bumped the surface three times, only the third (final) touched site could be studied [*Note for the reviewers: a reference will be added here after the first series of articles on Philae results are published*].

Among five classes of locomotion: wheels, tracks, legs, body articulation, and non-contact locomotion [13], hopping (a non-contact class of locomotion) is one of the most efficient ways of manoeuvring among obstacles that are much bigger than the robot itself, granting access to planetary areas so far inaccessible for conventional rovers. Hoppers may be considered as valuable alternatives to

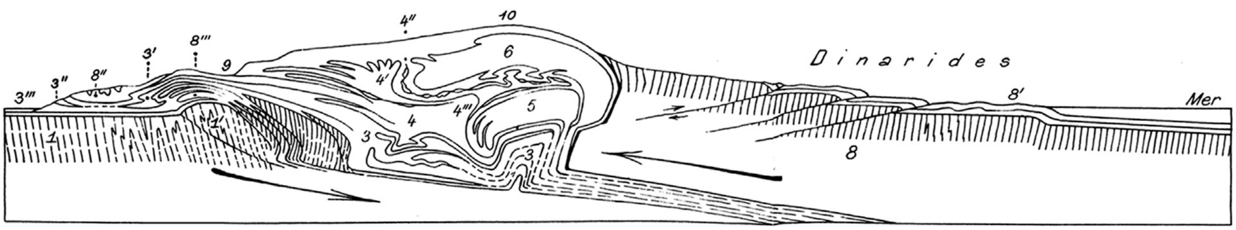

Fig. 1. One of the most astounding achievements of field geology: west–east geological profile across the Alps, an excerpt of an evolution scenario of the Alps (one of the most complex terrestrial orogens), proposed by Swiss geologist Emile Argand [14]. The modern geological and geophysical works have remarkably confirmed this interpretation. It is especially consistent with plate tectonics, which was theorised 51 years later. Mountain belts having structures similar to the Alps are not expected, in our current understanding, on the other planetary bodies considered in this article, but layered mounds such as Aeolis Mons (aka Mount Sharp) in Gale crater and the slopes of bedrock in Valles Marineris on Mars, as well as crater central peaks, are examples of geologically complex mountains that should be studied using a similar approach. Explanation of numbers: 1: basement (1′: basement deformed by the alpine orogeny); 3: foreland basin (3′, 3′′, 3′′′: migrated foreland basins); 4, 4′, 4′′, 4′′′, 4′′′: elements of the frontal cordillera; 5: internal crystalline massifs nappe; 6: second cordillera and Dent-Blanche nappe; 8, 8′, 8′′, 8′′′: Apulian units (8′′, 8′′′: transported onto the European tectonic plate); 9: drainage controlled by tectonic fabric; 10: Structural top of the western Alps.

landers and rovers for the exploration of Mars and the other Solar System bodies of smaller dimensions, allowing operations that both landers and rovers would do, with access to planetary mountains and controlled displacements at the surface of any body, including the smallest ones.

Hopping is a fast, and the main, locomotion system of many animals, sometimes with impressive efficiency. For instance, a study of two galago species have shown that they accumulate potential energy during a 1/10 s to 2/10 s, the instantaneous release of which produces up to 55 N [15], which given the weight of adult animals, ca. 400 g, should be enough (16.5 m/s) for galagos to escape the gravity field, if latitude-varying centrifugal forces and tidal forces are neglected, of Phobos (11.4 m/s on average) and Deimos (5.5 m/s on average), asteroid Eros (10.3 m/s on average) and by far, many asteroids such as Toutatis (1.9 m/s on average) and Itokawa (0.2 m/s on average), and cometary nuclei such as Tempel-1 (1.4 m/s on average) and Churyumov-Gerasimenko (1 m/s on average).

Humans have also found that hopping is a natural way of moving on the Moon, as illustrated by the conversation between astronauts Eugene Cernan and Harrison Schmitt during the Apollo 17 mission (corrected transcript from the Apollo Lunar Surface Journal by Eric M. Jones):

167:09:45 Cernan: (Doing long, two-footed hops) This is the best way for me to travel. Uphill or downhill.

167:09:48 Schmitt: What's that?

167:09:50 Cernan: Like this. Two-legged hop.

167:09:53 Schmitt: There seems…Yeah.

167:09:54 Cernan: And on level ground, I can skip. I don't like that loping thing.

167:09:59 Schmitt: Oh, the loping's the only way to go.

167:10:01 Cernan: Well…See, when I'm on level ground, I can skip. But this two-legged thing is great! Man, I can cover ground like a kangaroo!

This article presents an innovative type of hopper, named *hopter*, a robotic platform that is to replace a field geologist on moderate to ultra-low gravity solid bodies that combines the ability of climbing (and climbing down) scarps by following the most appropriate path, and recovering in case of fall, slip or blocking, as a geologist would do in mountains, but also jump to rock benches or beyond obstacles that are many times its height. It focuses on hopter definition and categorisation as well as examples of potential geological applications. The mechanical design is described in detail in a separate paper.

2. The HOPTER concept

2.1. Solar System exploration hopping platforms: state-of-the-art

Several approaches for space hopping have been investigated so far ([16,17]), some designed for ultra-low gravity bodies (Fig. 2a–e) and some for small planets like Mars (Fig. 2f–i), with only a few implemented in space missions. The Phobos-2 mission (1988) PROP-F hopper (Fig. 2a) possessed a dedicated leg for accumulation of jump energy and special arms to flip it to the initial jumping position, following a ballistic arc [18,19,17]. The MINERVA hopper (Fig. 2b) deployed from Hayabusa had a cylindrical shape and a system of two actuators of which one played a role of a torque wheel to induce hopping force, and the second determined hopping direction [20]. Hayabusa-2 includes three MINERVA-2 hoppers and a MASCOT hopper. MASCOT (Fig. 2c) originally was to be a hopper actuated by an arm movement, but eventually the arm was changed to an eccentric reaction wheel allowing to perform multiple scientific measurements in different locations during its short operation life time of 16 hours [21]. The Hedgehog concept takes also advantage of reaction wheels, but they introduced three wheels orthogonal to each other. As a result, it is considered as a spacecraft/rover hybrid. Its cubical shape equipped with spikes all around makes it capable of performing pivoting, slipping and hopping (Fig. 2d) [22]. The Comet Hopper (CHopper), considered for a NASA Discovery Program mission, had to hop a couple of times on comet 46P/Wirtanen (Fig. 2e) at different times during descents to the surface of the comet [23]. On bodies with higher gravity field (e.g., Moon and Mars), the released kinetic energy needs to be substantially higher.

The large Mars Reconnaissance Lander (MRL, ~500 kg; Fig. 2f) uses a radioisotope stored in thermal rocket engine and repeatedly compresses CO_2 and discharges it through thrusters [24,25,26]. It takes advantage of performing short, controlled ballistic flights to achieve distances of c.a. 1.5 km, giving the capability to cross terrain inaccessible to conventional rovers, but in fact still cannot access those since it still requires flat terrain for landing. The Mars in-situ Propellants Rocket (MIPR) hopper has objectives similar to the MRL but uses solar power to react atmospheric CO_2 into O_2 and CO [27]. The 1.3 kg elastic cage design (Fig. 2g) protects the payload and mechanism by multiple bended metal strips arranged as ribs. Jumping is achieved through cage compression and sudden release along the vertical axis [28]. The partially prototyped design of Martian hopper with Shape Memory Alloy (SMA) actuator (Fig. 2h) is tetrahedron-shaped. The jumping mechanism is a unique actuator in contact with the ground attached to the tetrahedron chassis in which the payload is to placed. After each jump the hopper flips back to the starting position. The SMA actuator is driven by the diurnal temperature gradient, and because of the single actuator, the angle of jump is fixed [29]. As advocated by its shape, the Spherical Mobile Investigator for Planetary Surfaces (SMIPS, Fig. 2i) primarily rolls, and does this by offsetting its centre of mass [30]. Negotiation of small obstacles by jumping may be achieved by quick acceleration of the internal pendulum, expansion and release of the ball in the direction of its telescopic axis, or increase of the ball internal pressure and release the gas through nozzles.

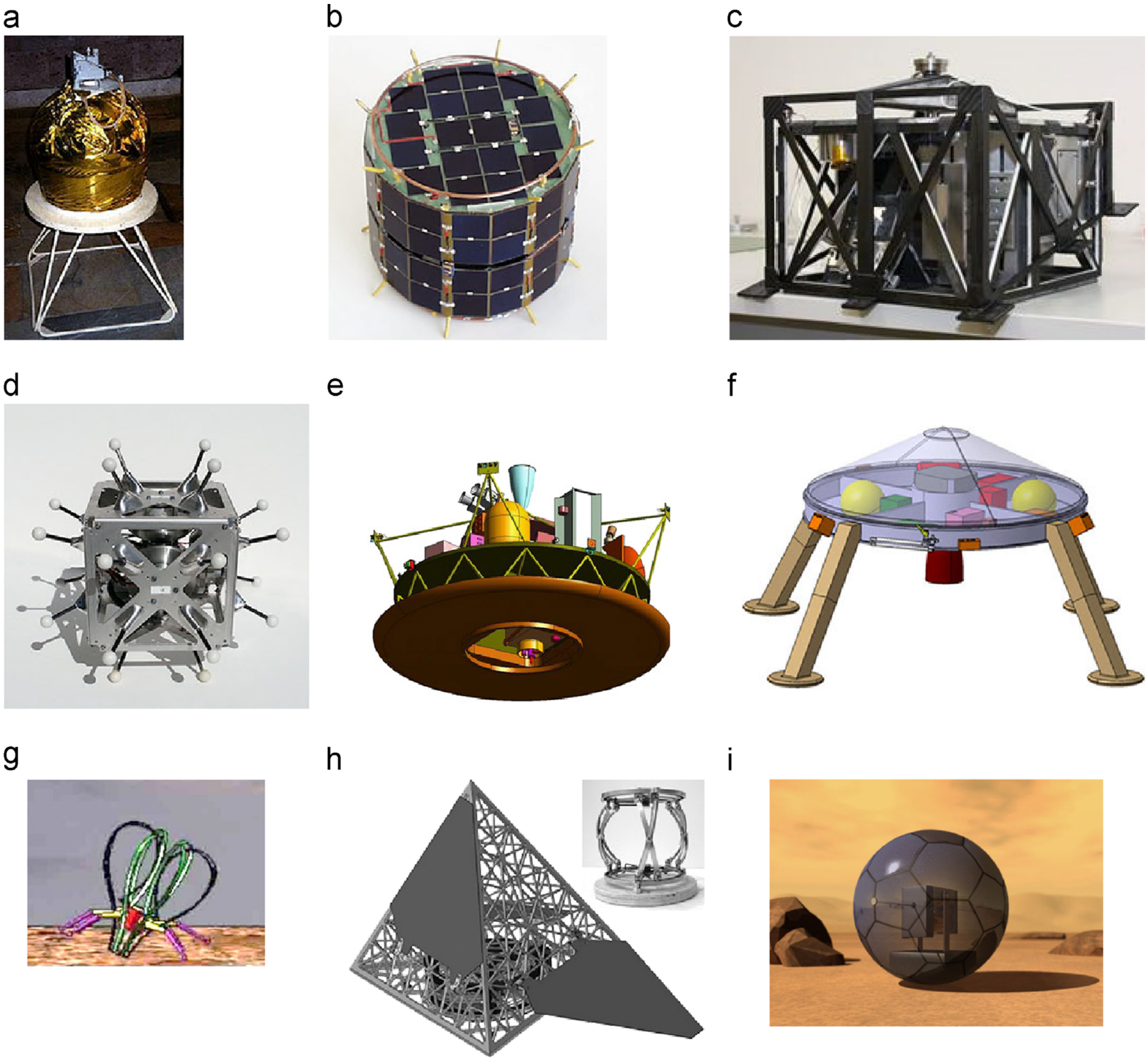

Fig. 2. Previous hoppers for the study of low-gravity Solar System bodies: (a) Phobos hopper [31]; (b) MINERVA [20]; (c) MASCOT [32]; (d) Hedgehog [22]; (f) Comet Hopper [23]. Planetary hopper solutions: (f) Mars Reconnaissance Lander [26]; (g) Elastic cage design [28]; (h) Hopper with SMA Actuator [29]; (i) Spherical Mobile Investigator for Planetary Surface [30].

2.2. HOPTER design

We define HOPTER, an acronym for Highland Terrain Hopper, as a new category of locomotion systems based on controlled jumping aiming at studying the surface, subsurface, and environment of low and ultra-low gravity bodies (Fig. 3). Hopter mechanical design is detailed in another paper. The currently designed hopters are small and light locomotion platforms (Table 1) including miniaturised instruments [33,34,35]. The main system, located in the central part of the platform, controls three independent electromagnetically driven actuating legs designed to propel the hopter to a specified place located at a maximum distance that depends on the value of the acceleration of gravity (or escape velocity) of the explored body, and a maximum jumping height that also scales with gravity. The considered mechanism is designed to allow a maximum jumping height of 4 m on Mars

Fig. 3. Artist's view of a hopter in a Valles Marineris-type landscape (no vertical exaggeration). The maximum jumping height on Mars with the currently considered mechanisms is anticipated to be 4 m.

Table 1
Hopter design parameters.

Envelope diameter	60–70 cm
Envelope height	30–40 cm
Central disk diameter	40–50 cm
Central disk height	8–10 cm
Total mass	8–10 kg
Payload mass	2–3 kg
Battery voltage	12 V
Electric charge	7 A h
Total energy stored	300 kJ
Energy accumulated in a single actuating leg	40–50 J
Maximum number of jumps with full battery charge	1000[a]
Maximum jumping height (scales with gravity)	Mopters and kbopters: 4 m on Mars, 9 m on the Moon, 22 m on Pluto, 53 m on Ceres, 130 m on Enceladus Phopters: no limitation

[a] Assuming 50% efficiency.

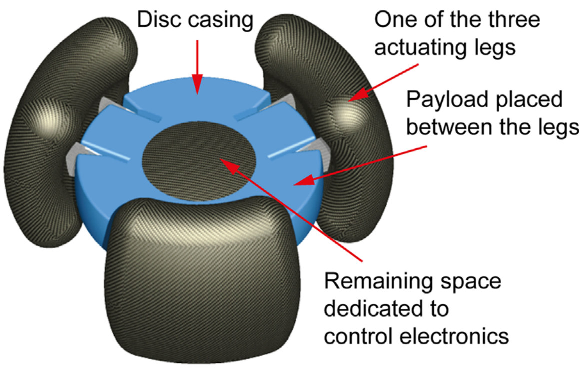

Fig. 4. Hopter anatomy.

(Table 1). The battery, charged by solar panels if the studied body is close enough to the Sun (see next section), has an autonomy of 500–1000 jumps without recharge, which allows for a nominal horizontal travel distance of 5 km. This distance is anticipated to be increased by several hundred percent by battery recharge, making the distance currently travelled by opportunity (> 40 km) conceivable. The main system is located in the central part of the platform, and the three inter-leg spaces are left for payload (Fig. 4). Power is supplied by a battery that can be recharged by solar panels that would be located at the top and bottom of the platform and protected against impacts by an overlying grid (not displayed on Fig. 4). The hopter is fully symmetric, which allows to increase the variety of displacement modes. Many risky displacements are made possible by robot symmetry and leg configuration; they make risky scientific objectives achievable. In case of failed jump, the hopter remains operational for a next attempt. One leg at least is staying in contact with the ground and can be used to reposition the hopter and prepare it for a new jump.

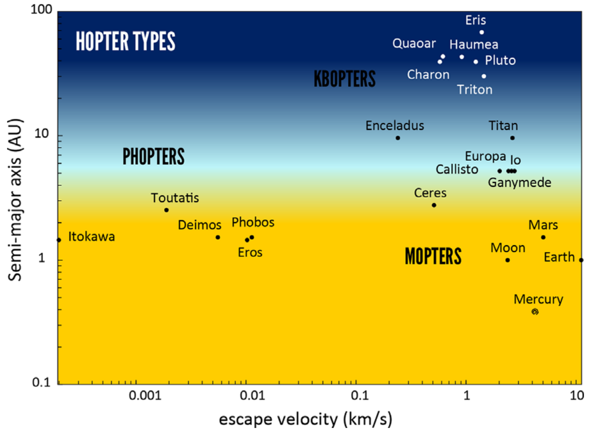

Fig. 5. The main hopter categories depend on escape velocity (centrifugal and tidal forces are neglected) and insolation conditions. Yellow background indicates the region where battery recharge by solar panels is useful. (For interpretation of the references to color in this figure legend, the reader is referred to the web version of this article.)

2.3. Categorisation

Most solid Solar System bodies can be explored by hopters (with the exception of Venus due to its atmospheric pressure), but adaptations may be required, depending on escape velocity and solar radiation (Fig. 5). We define three hopter categories:

- *Mopters* are adapted to the Earth, Mars and the Moon. On Mercury, the temperature conditions, up to more than 400 °C, require specific cooling systems that consume additional power. Mopters may also be adapted to the study of some of the giant planets' satellites.
- *Phopters* are adapted to bodies having an escape velocity which is low enough for mopter mechanisms to be endangering for a hopter to go back to the ground surface, such as Phobos, Deimos, asteroids, and cometary nuclei approaching the Sun to a distance approximately longer than the distance between the Sun and Mercury. Less energetic mechanisms are required.
- *Kbopters* are adapted to the ultra-low temperatures (typically 30–40 K) that are encountered at the surface of KBOs, and cometary nuclei at similar distances to the Sun. They require technological adaptations accounting for such temperatures.

All the hopters are powered by batteries, but those close enough to the Sun can be recharged through solar panels, whereas more distant hopters receive much less solar radiation. Kbopters and some phopters are concerned; however, for the phopters in the inner Solar System, the absence of solar panels is anticipated not to be an issue due to the extremely low force required for jumping and its velocity not to exceed the escape velocity of the explored body.

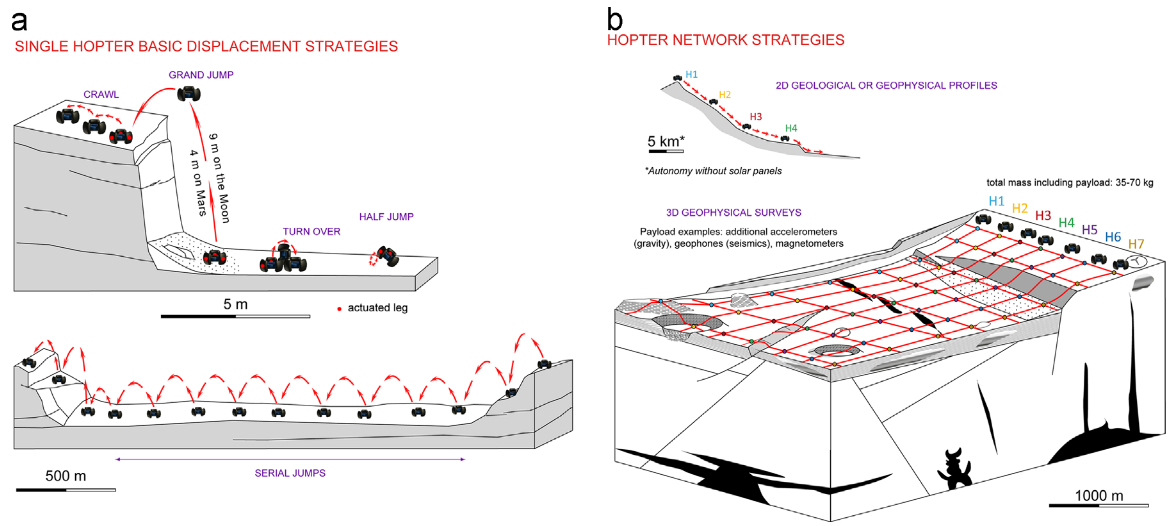

Fig. 6. Hopter displacement strategies (scales are for landscapes, hopters are not drawn at scale). In addition to the various Hopter displacement possibilities (a), low mass allows several hopters to be dropped at a study site for networking, using duplicated or complementary payload (b).

2.4. *Displacement strategy*

The independence of the three actuating legs makes several displacement modes possible, depending on terrain configuration, instrument location and orientation, and scientific objectives (Fig. 6a). In case a hopter falls upside down, the full symmetry of the platform and legs make the next jump possible without implementing a recovery procedure; in case of failed jump resulting in an unexpected hopter orientation, some of these modes are also adapted to reposition the hopter to an appropriate position for the next jumps due to the independence of the legs and their ability to adjust the released energy of each separately.

The independent release of graduated energy allows 4 displacement strategies to be implemented, depending on the scientific objectives as well as the local terrain configuration. A *grand jump* is adapted to climbing cliffs or jumping over obstacles (Fig. 6a). This way mountain outcrops can be investigated, as well as jumped over to access, for instance, flat terrains that are not accessible to rover because the landing ellipse would be too large. For local investigation of a promising small outcrop, for instance to investigate rock structures exposed on a steep of vertical slope, crawling may be adapted; if an instrument is not properly aligned with an outcrop for measurements, *platform turnover* may solve the issue. Platform turnover may also be a solution before activating an instrument the system of which cannot function properly when upside down. A *half jump*, consisting in platform rotation of not more than a few tens of degree in a vertical plane about the end of one platform foot, by actuating the two other legs, may end up with hopter fall to a position that is slightly different from the initial position, which may be helpful to slightly reorient the hopter to improve observation or measuring conditions, and may also be useful for stereo image acquisition. If the hopter is on a slope, such a limited rotation jump will be associated to a torque that will reorient the hopter to a predictable direction.

Hopters can be used in exploration mode, as shown above, but also in cruise mode. In order to access outcrops tens to hundreds of metres away separated by flat and smooth terrain, *serial jumps* (without any human operation between jumps) may be programmed. Although automatic programming of many jumps is technically achievable, jumping accuracy would significantly decrease after a few jumps. It appears therefore that a strategy consisting in series of a few automatic jumps separated by hopper position checking by staff is the fastest safe way of crossing terrains when geological observations are not planned, corresponding to a travelling distance of ca. 60 m/day on Mars or ca. 150 m/day on the Moon.

These strategies make possible independent investigations of study sites. One of the most innovative aspects of the hopter concept is that due to the low mass and cost of the platform, investigations of a site of high scientific interest using multiple platforms dropped in the same area, open the opportunity of networking. At the same study site, multiple hopters carrying different but complementary payloads may undertake a comprehensive field study. Alternatively, duplicate payload makes it possible conduction of two-dimensional *geological or geophysical profiles* the same way geologists do in the field on Earth (Fig. 6b). Each hopter may be in charge of a segment of the profile, for a given hopter autonomy, the length of the full profile depends on the number of hoppers. Profiles tens of kilometres long may be studied. Furthermore, *gridded geophysical surveys* can also be conducted for subsurface prospecting and reveal the three-dimensional properties and structure of the subsurface, the same way gravity, magnetic or seismic surveys would on Earth.

The displacement performance of hopters may be evaluated against the performance of Martian rovers on flat terrains, for instance Curiosity, the most sophisticated Martian rover to date. The calculations below are illustrative only. The situation considered here is that the robot is moving on a terrain which is flat but with useful geological observations to make in its vicinity (layer attitude

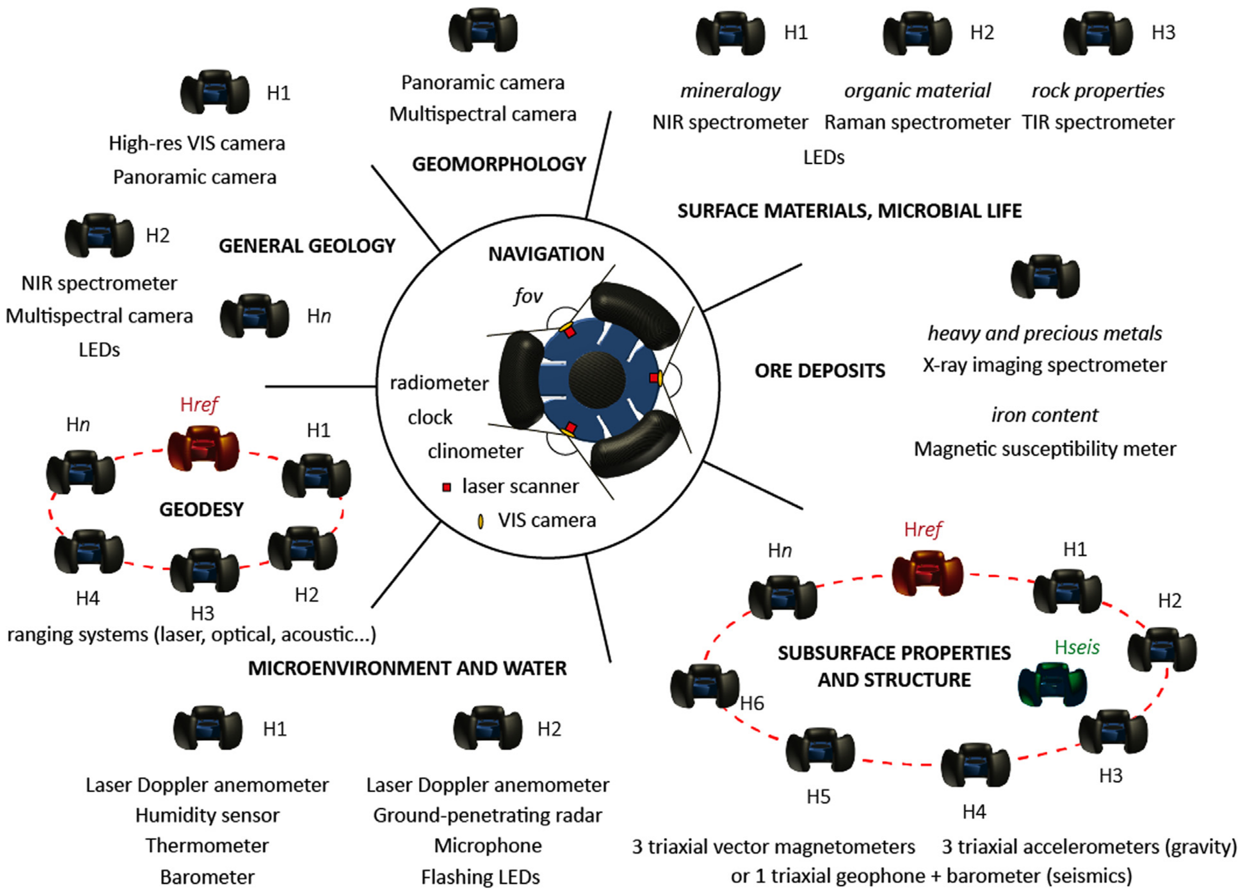

Fig. 7. Examples of hopter mission goals and adapted miniaturised payloads. The navigation subsystem (seen at the centre) is common to all missions (*fov* is for field of view). For geodesy, no additional instrument is required. For other mission goals, additional instruments are required, and sometimes additional hopters (numbered H1 to H*n*), plus a reference station (H*ref*) for geodesy and magnetic surveying. Shallow seismic experiment may use a dedicated hopter for seismic noise production (H*seis*).

determination, analysis of faults or rock fabric, variations in sedimentary deposition, determination of lava flow direction etc.), resulting in a low displacement speed. The average travel distance of Curiosity, of mass 900 kg, over 2 years is $T=10$ m/day. Terrain coverage per unit mass and day is $C=0.011$ m/kg/day. The same distance may be easily travelled by a hopter: 10 m corresponds to 3 or 4 jumps, which on flat terrains may be achieved in a single day, potentially by serial jump programming (Fig. 7a). For a hopter of maximum mass 10 kg including payload, $C=1$ m/kg/day, i.e. a 90 times more than Curiosity. Assuming that the useful observations (panoramic views excluded) around Curiosity and a hopter are at a maximum lateral distance of 4 m, the useful surface area for field observations covers 40 m^2 daily, corresponding to 0.09 m^2/kg/day for Curiosity and 8 m^2/kg/day for a hopter. For similar platform mass, 900 kg, the 0.09 m^2/kg/day for Curiosity transforms to 620 m^2/kg/day for an orthogonal mesh of 90 hopters of mass 10 kg. These calculations illustrate that in any given area that is accessible to rovers and hopters, the mobility of hopters for a similar launch cost is much higher, making possible hopter ferreting out with high mobility before selecting target sites for detailed investigation.

2.5. Payload and mission topics

Each hopper may carry up to 3 kg of payload (Table 1). In order to save space and weight, as well as make hopters more robust and less prone to destabilisation on sloping the ground, the main system and payload systems may be highly miniaturised and designed simultaneously in a non-conventional way in order to mutualize as many components as possible.

This mass basically allows one hopper to conduct an independent study with at least one or two main instruments (for instance, spectrometers) in addition to a number of very light instruments (cameras, temperature and humidity sensors etc.). Loading a hopter as much as possible may however not always be desirable, for instance in case of magnetic field investigations, as detailed below, for which magnetic noise within the platform is to be kept as low as possible. In general, a multifunctionality approach for the payload and main system components is favoured, in which for each hopter a scientific task or objective is assigned, the system and subsystem structures are invented, and feasibility is investigated.

Although microelectromechanical systems (MEMS) technology usually features extremely small components, the miniaturisation driver is not saving mass, but money, or increasing performance, e.g., a sensor's sensitivity or an actuator's displacement resolution. For this reason, systems employing MEMS components might, to a large extent, contain also conventional, mass-produced components, as the opposite is not justified, and, hence, be as heavy as systems based on conventional technology. Here, mass is of essence, and part of the solution is integration on different levels. At the lowest level, microdevices can be integrated on chip, with little or no mass penalty. For instance, two (or ten or a hundred) elements for magnetic field measurements can be put on the same chip as one. On the next level, more or less naked chips, or their equivalents, can be put on the same carrier, sometimes referred to as multi-chip modules. By this, e.g., signal handling and power supply, as well as substrates and encapsulation can be shared, and the mass added by the MEMS-based subsystem can approach that of the MEMS components themselves, which is usually a couple of grams.

A next step may be using components for more than their primary purpose. This is a kind of multifunctionality, sometimes strived for, but not often achieved, as it asks for system design aspects from very different disciplines. Good examples of these approaches are given in the ÅSTC's NS-1 concept, a nanosatellite based on microtechnology [36]. Whereas other nanosatellites, like microsatellites and even picosatellites, rarely contain MEMS components, this one does, and, furthermore, it accommodates naked commercial off-the-shelf (COTS) electronics components in multilevel multi-chip modules made of silicon, the standard MEMS material, and uses these modules to mechanically support the spacecraft chassis [37], aid in the craft's thermal management by active IR emitter coatings, or to the communication subsystem by housing patch antennas, or all of it [38]. An endeavour along the same lines, but more similar to the hopper, is the SMIPS spherical rover ([30] and Fig. 2i), also from ÅSTC. It does not exhibit the same massive implementation of MEMS devices as NS-1, but most of its body is a multilayer, multifunctional shell with embedded components and circuitry, harvesting solar energy, protecting the inner parts, and constituting the tyre at the same time.

Multiple hopper investigations may be conducted using duplicate or complementary instruments serving various scientific observation and measurement scenarios, as illustrated with examples on Fig. 7, using the concept of fractionated spacecraft [39], here renamed fractionated explorer. Some instruments are required for navigation and may be used for general scientific purposes. For instance, obtaining accurate topography around a hopter is mandatory for navigation, and may be performed by photogrammetric processing of camera images obtained either by more than one hopper, or a single hopper, complemented by laser scanning. The resulting topographic information is helpful for any scientific application, starting with geomorphology and, using a hopter network, geodetic measurements and control point network determination. For geodetic measurements, one of the hopter is to be used as an immobile reference station (H*ref*, Fig. 7) performing measurements against which all the other measurements are calibrated.

The analysis of surface rocks may be obtained by combining various instruments onboard two or three hopters, in addition to optical cameras placed on the hopter sides, top and bottom. Mineral composition may be obtained by near-infrared spectroscopy using e.g. a Fourier transform spectrometer operating in the wavelength range 1–5 μm. Composition information may be complemented by data from luminescence from the ultraviolet to the red domain, using LEDs of specific colours mounted on the camera (the LEDs may additionally be used to view around the hopper during night-time if required) as well as Raman spectrometry [40]. Organic material and biological organisms may be detected and identified using the two latter techniques [41,42]. Rock porosity may be inferred from thermal inertia obtained from infrared data. Exploration of ore deposits such as iron and heavy metals may be conducted by analysing the anisotropy of magnetic susceptibility [43] and X-ray imaging spectrometry [44], respectively. Studies of the microenvironment may be conducted to monitor weather, observe the ground, and probe the underground. The weather station may record basic parameters such as pressure, temperature, and humidity, and also LEDs for detecting dust [45,46]. Camera recording the surrounding atmosphere at night illuminated by flashing LEDs would allow tracking dust particles and determine their velocity and three-dimensional motion. In order to monitor wind speed, a minimum a two hoppers are required for a laser Doppler anemometer to operate. Ground ice detection, using a ground-penetrating radar, would reveal materials having contrasting dielectric constant, and would be efficient at detecting pure H_2O ice and CO_2 ice. A microphone would allow to detect noisy geologic processes such as glacier ice cracking or mass wasting.

Hopters are adapted to classical regional geology surveys, including completion of geological profiles tens of kilometres long, as fruitfully done on Earth for many decades (Fig. 1). A minimum of two hopters having a complementary payload may harvest geological information pertaining to tectonics, sedimentary geology, mineralogy, and rock identification. The hopter optical cameras and clinometer, used in the navigation subsystem to evaluate the current hopter attitude and plan jumps, are here critical instruments for the determination of the orientation of geological layers in front of rock outcrops as field geologists are used to do, or from the distance. Combining geological surveys the same way geologists do on Earth may lead to geologic maps with as many details as terrestrial geologic maps.

Various types of geophysical surveys may be conducted. Typically, geophysical surveys, as well as geodetic surveys as described in Section 3.3, fully benefit from the networking capabilities of hopters. This certainly adds complexity to scientific objectives for which one or several independent hopters are operating. This complexity, however, is not as much a consequence of required technological developments, which have been undertaken by various groups for other purposes, as a consequence of data processing for noise reduction and dedicated processing schemes inherent to networking. The potentiality of networking with hopters is illustrated below with examples in gravimetric, magnetic, and seismic surveying.

Measuring the three components of the gravity field and their variations can be done on a single hopper using three perpendicular accelerometers located in each of the three hopter legs, similar to a technique developed for underwater gravity field measurement [47]. This way subsurface density anomalies may be imaged during jumps. Several hoppers carrying this payload distributed over a grid pattern (Fig. 6) would be able to conduct a 3D gravity survey and locate features such as magmatic intrusions and ice lenses.

Similarly, the three components of the magnetic field and its variations may be studied at very low weight using miniaturised magnetometers. Benefitting from the development of this kind of instruments for picosatellites (also referred to as CubeSats), where a conventional, high-performance, three-axial magnetometer would have roughly the mass of the entire craft, the hopper can be equipped with microsensors equal in merit, but a few thousandth the mass, including electronics [48,49]. Based on thin film technology, and given their small size and simplicity, these sensors are very robust, and can be integrated with the vehicle with few constraints. However, contrary to the rest of the payload, these sensors are likely to be disturbed by the hopper's locomotion and communication subsystems, wherefore mounting on or inside the vehicle requires that measurements are carefully synchronized with these, or that the signal can be filtered.

Hoppers may be equipped with 3-axis vector Hall-effect magnetometers [50], located between each hopter arm, that would be activated while jumping. Measuring the magnetic field during a jump the trajectory of which is accurately prepared allows magnetic anomalies to be identified, and from comparison with a magnetic model calculated at 1 A/m, absolute magnetisation can be retrieved [51]. Hopter magnetic survey may thus be used to reveal the magnetic stratigraphy, the location of magnetic bodies, as well as the absolute value of the magnetic field on the ground. For a magnetic survey, a reference station (*Href*, Fig. 7) is required to record potential evolutions of the external magnetic field during the measurements carried out by the other hopters.

A seismic network, the Apollo Lunar surface Experiment Package, was deployed at the surface of the Moon and operational between 1969 and 1977, with 4 stations recording more than 12,000 events [52]. On Mars, the Viking seismic experiment included two seismometers onboard the two Viking landers [53]; however, only the Viking Lander 2 experiment was successful and it returned data for 19 months. Since that time, in spite of several attempts (Roscosmos Mars'96, ESA/NASA MESUR-MARSNET, ESA/NASA INTERMARSNET, ESA/CNES Netlander, Humboldt payload of an early version of ExoMars), seismic stations could not be deployed successfully on other Solar system bodies until today. The NASA/InSight SEIS experiment [54], planned to land on Mars in 2016, includes two 3-axis sensors, the VBB very-broad-band seismometer (e.g., [55,56]) and the SEIS-SP, MEMS-based short-period seismometer (e.g., [57,58]). In spite of a single station, detection of major layers to a depth of hundreds of kilometres is expected using VBB [54,59] and the current impact rate at regional-scale determined by SEIS-SP [60]. Building on the achievements of SEIS, a network of hopters carrying 3-axis sensors, similarly MEMS-based, may be optimised to obtain data that complement those obtained by the SEIS package. For instance, a hopter network may be able to identify seismic layers and image the subsurface to depths of tens of metres to tens of kilometres, complementing the data that will be obtained by the NASA InSight mission. With a landing mass of ~350 kg, InSight is 35 times more massive than a hopter, suggesting that for the same launch mass cost many hopters may be launched.

Seismic networks deployed from hopters would have to face several challenges, such as hopter coupling with the ground to obtain a high seismic signal from the seismic source, and reduction of local noise. Technical studies of required hopter leg surface microstructure as well as identification of the most appropriate mass and mass distribution within the hopter will be required in order to maximise hopter coupling with the surface. Noise arising from local near-surface irregularities and external perturbations (e.g., wind shaking; [61]) is typically removed on Earth by acquisition of a large number of seismic stations and records. Noise from local winds is to be expected on Mars; an encouraging observation from the Viking mission, however, is that the background seismic noise should be low and no other significant noise source has been identified [53]. Wind noise may be attenuated by carefully selection of the hopter site and attitude [62] with the help of barometric data [63]. In the InSight mission, the SEIS experiment is deployed outside the lander with a robotic arm and protected with a wind and thermal shield. Due to their small size and proximity to the ground, each hopter could be considered as a shielding platform hosting the seismology instrumentation. Processing of data from a swarm of hopters would contribute to further noise removal. Adaptation of seismometer frequency range to the interesting seismic waves anticipated to be detected in the geological medium is another challenge. To assess this challenge, we address below the possible causes and sources of quakes, as well as the frequency range of their seismic signature and the type of geological information that can be extracted.

The causes of quakes on other Solar System bodies include impact cratering ([60,64] on Mars), planetary cooling (e.g., [65] on Mars), tides (e.g., [66] on the Moon), perhaps active volcanism (hypothesised on Mars by [67]) and active crustal tectonics (hypothesised on Mars; e.g., [68]); and plausibly on Mars, surface processes such as landsliding, rock fall, and glacier evolution. Processing of seismic records could reveal hypocentres, such as impact sites, the depth of major planetary discontinuities such as between the crust and mantle (see [69] for a discussion on this boundary on the Moon) and the mantle and core [70]; active volcanoes, faults, active glaciers and areas of active mass wasting. It could discriminate between these sources and could even reveal some characteristics of the detected geologic processes through advanced techniques of wave analysis developed for terrestrial applications, for instance magma conduit propagation and associated shear failure

[71], hydrothermal processes associated to magmatic events, and volcanic tremors; rockfalls [72,73], granular flows [73,74] and avalanches [75]; glacier calving [76,77] or stick-slip motion of glaciers on bedrock [78]. Heterogeneous bodies undergoing significant tidal effects should also reveal seismic activity which is not yet characterised. Wave analysis could also inform on the discontinuities along the ray paths, such as sedimentary stratification (especially sedimentary basins on Mars; e.g., [79]) down to the underlying basement, the shape of magmatic intrusions, and the base of regoliths, the thickness of which could be estimated. Basalts are very frequent in the crust of planetary bodies, which causes problems due to scattering and loss of transmitted seismic energy in basalt (e.g., [80]). This problem may be mitigated in various ways, especially if the basalt is located at depth, using a low frequency seismic source (<10 Hz, e.g., [81]) and if other geophysical data can be obtained for joint inversion (e.g., [82]).

MEMS-based accelerometers are ideally adapted to the low payload mass requirement of hopters. Having capabilities equivalent to conventional short-period geophones, higher in some respects [83,84,85,86,87], technological developments allow to gradually replace broadband geophones by improving the signal toward low frequencies [88,89]. Thermal MEMS [90] may be alternatively considered. Coupling hopters equipped with 3-axis seismic sensors with a ground-hammering dedicated hopter operating as a seismic source (H*seis*, Fig. 7) may reveal the shallow subsurface structure. Having the hopters carrying seismic sensors move along a grid as on Fig. 6b may provide a 3D image of the crust over a volume depending on the network geometry and the MEMS capabilities.

The MEMS-based accelerometer of the InSight mission covers the 0.05–40 Hz range, complementing and somewhat overlapping the 0.005–1 Hz range of VBB. Altogether, they cover the whole range of natural quakes known on Earth. Nevertheless, the single station of InSight will not permit the majority of the abovementioned geological measurements and interpretations, which do require a network of stations. Which are the processes that could be studied by a network of hopter stations carrying only MEMS-based sensors? In terrestrial applications, there operational range is from 0 to 800 Hz, but the highest values are obtained in boreholes only [86]; and in environments without human activities, such as the Martian environment, signals at less than 5 Hz are hardly detected [91] due to noise floor [92]. The latest generation of MEMS-based accelerometers, however, has a sensitivity in low frequencies increased by a factor of 10 [88], which may be even improved to below 1 Hz by denser spatial sampling [93]. The ground noise, which partly depends on wind and atmosphere conditions, may be different on Mars, depending on the selected geographic sites and seasons. Seismic signals that should be identified and characterised by a hopter network due to a frequency higher than a few Hz include tectonic deformation generated by underground magma motion (up to 40 Hz; [71,73]) such as dyke emplacement (e.g., 1–15 Hz was recorded at Etna; [94]) and perhaps tremors (up to 3–4 Hz; [71]) that could be monitored; rockfalls (up to 15–20 Hz; [72,73]); landslides, avalanches and granular flows in general (up to at least 15 Hz; [73,75,74]); glacier stick-slip motion on bedrock (up to 5 Hz; [78]) and calving for quakes of low magnitude [76]. Detection of seismic surface and body waves that would have properties of typical of plate-boundary displacements on Earth would benefit from future advances in MEMS-based technology due to their low frequency (0.05–0.1 Hz for earthquakes of moderate magnitude and less by one or two orders for earthquakes >8). In the absence of plate tectonics, very strong earthquakes having such properties are not expected on other planetary bodies, although they cannot be ruled out. Volcanic tremors and hydrothermal processes associated to magma emplacement, as well as glacier calving would also benefit from future advances in MEMS-based technology toward lower frequencies [71,76,77].

It is anticipated that hopter investigations not only complement rover and lander investigations, but also propose a new way of thinking acquisition of planetary exploration data, very much inspired by the way earth science research is conducted for terrestrial studies. Hopters can be sent as piggy-back robots on future missions that include a rover, similar to the NASA/Mars 2020 mission, a lander similar to the Roscosmos/Luna-Glob mission (currently scheduled in 2024) or a lander network such as the ESA/INSPIRE Mars network project, the International Lunar Network (scheduled to start in 2018), but also airplane-based scout missions to Mars and manned missions within the framework of the ESA/AURORA programme in which hopters can help access areas that are risky for humans. It could also be used for any future mission that would be designed to land on the surface of Phobos, Deimos, cometary nuclei, and asteroids.

3. Examples of scientific applications

3.1. Mars exploration: Valles Marineris

The usefulness of hopters for Mars exploration is illustrated by an example in the Valles Marineris canyons. This example is selected because a cross section in Valles Marineris would provide insight into the whole planet history. Although landing sites have been suggested for rover missions (e.g., [95]), the landing ellipse constrains the landing site to be very far from the Valles Marineris walls, where a very long geologic history is recorded, and restricts the observations to a few sedimentary units. Most of the geologic landscapes are not accessible to rovers indeed (Fig. 8).

Exploration of Valles Marineris could be conducted along a transect that would comprehend the crustal basement over a thickness of up to 10 km and the whole sedimentary pile filling the canyons, studying all the geological events from their imprint on the current geomorphology, their compositional effect of rocks, and their geophysical signature. A synthetic geologic cross-section of Valles Marineris is presented (Fig. 9a), mainly inspired from the eastern Candor Chasma (external layered deposits have not been identified in this area). The current distribution of HiRISE images does not allow a continuous transect to be analysed (Fig. 9b); nevertheless, like during terrestrial field work, good understanding of a given geologic ensemble is more likely to arise from multiple

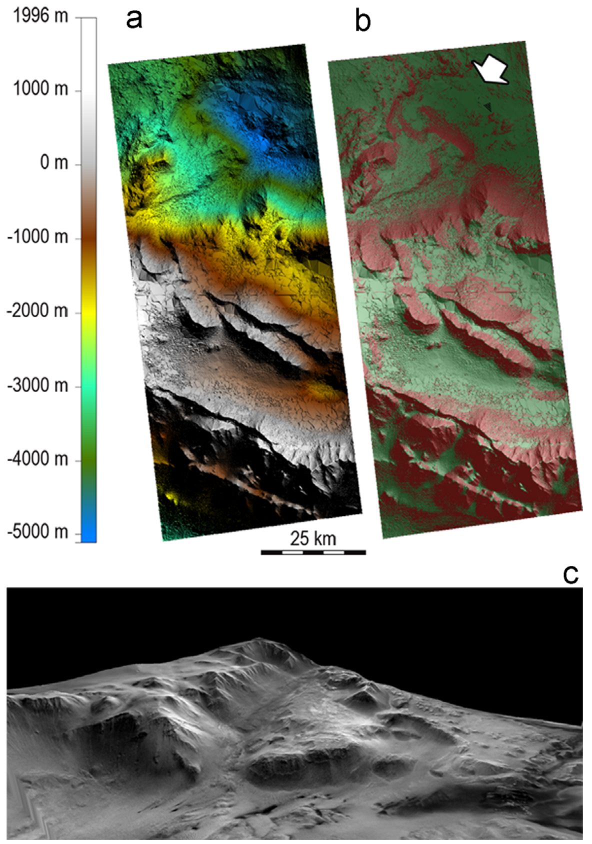

Fig. 8. Valles Marineris landscape (southwest Candor Chasma). (a): CTX shaded relief map; (b) Slope steepness map from CTX digital elevation model: the slopes $<30°$ are green and the slopes $>30°$ are red. The red areas are not accessible to conventional rovers, nor are the more gentle slopes and flat terrains surrounded by these areas. (For interpretation of the references to color in this figure legend, the reader is referred to the web version of this article.)

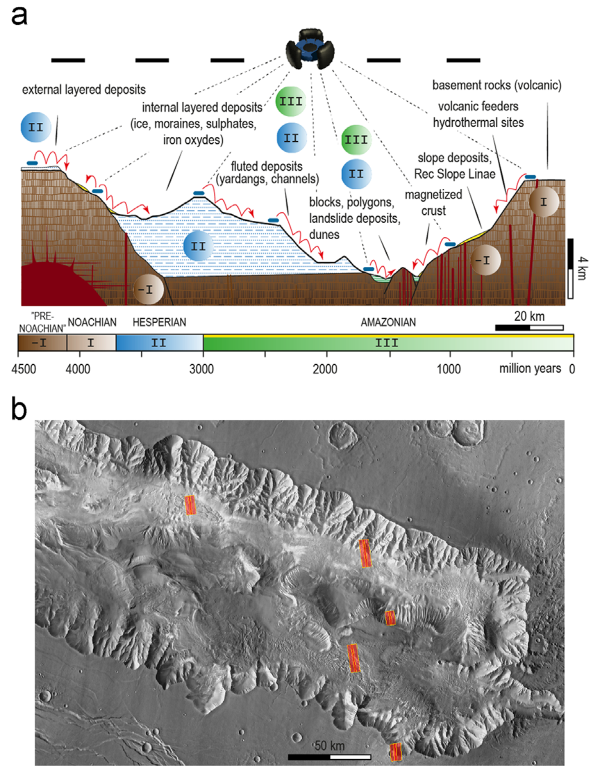

Fig. 9. (a) Synthetic Valles Marineris geologic cross section, mainly inspired from eastern Candor Chasma (external layered deposits have not been identified in this area; [102]); (b) location of the HiRISE images used for the fictitious transect analysed in Fig. 11. All the duration of the exposed geologic history of Mars can be studied in such a short cross-section; the use of the same instrument set at each observation site would make site-to-site comparisons conditions ideal.

profiles selected for key exposures than a single very long profile (e.g., Fig. 1).

Fig. 10 summarizes some key landforms in eastern Candor Chasma (Fig. 9b) that could be investigated using hopters but would not using conventional rovers. In this example, 2 hopters for regional geology, and an additional two (including a reference station) for magnetic surveying basement rock, would provide invaluable information to answer key scientific questions for better understanding the evolution of Mars: what is the thickness of the individual lava flows in Valles Marineris, which appears to be representative of the composition and structure of the uppermost Martian crust [96]? What can be inferred from the detailed analysis of the Valles Marineris chasma walls in terms of lava flow directions and emplacement modes [97,98,99] Are the lava flows fed by local dykes, are there indicators making it possible identification of their origin, how do they relate to Tharsis magmatism [100]? What is the absolute magnetization at the surface of the Martian crust? What is the nature of the magnetic reversals, some of which are recorded in the eastern Valles Marineris (e.g., [101])? Is there evidence of polar wander in the magnetic anomaly record on the ground that could have been generated by reorientation of the planetary rotation axis, following crustal or lithospheric loading in the Syria Planum-Tharsis area by cooling of voluminous early magmatism [103,104]? What is the composition and magnetization of the deep Valles Marineris basement observed underneath the lava flows [105]? Can graben border fault be identified along the walls, what is their kinematics, can their throw (e.g., [106,107,108]) be estimated? What is the nature of the Interior Layered Deposits (ILDs)? What is the proportion of sulphates, basalts, ice, and other components? Are the ILD sulphates observed to have formed from alteration of basalts in glacial conditions (e.g., [109,110])? The answers have consequences for the geological processes of the whole planet because very similar deposits are widespread on Mars, including in Gale crater [111] and others (e.g., [112]). What in situ landscape analysis tells us about the succession of climate periods since the Noachian? What is the thickness of the supraglacial till on fossil Valles Marineris glaciers, which may occupy as one million cubic kilometres [113]? What is the nature, origin and flow triggering mechanisms of the Recurring Slope Lineae (RSL) [114], observed in Valles Marineris [115] and many other regions of Mars [116], can they play a role in planetary habitability given the composition [117] of the flowing liquids?

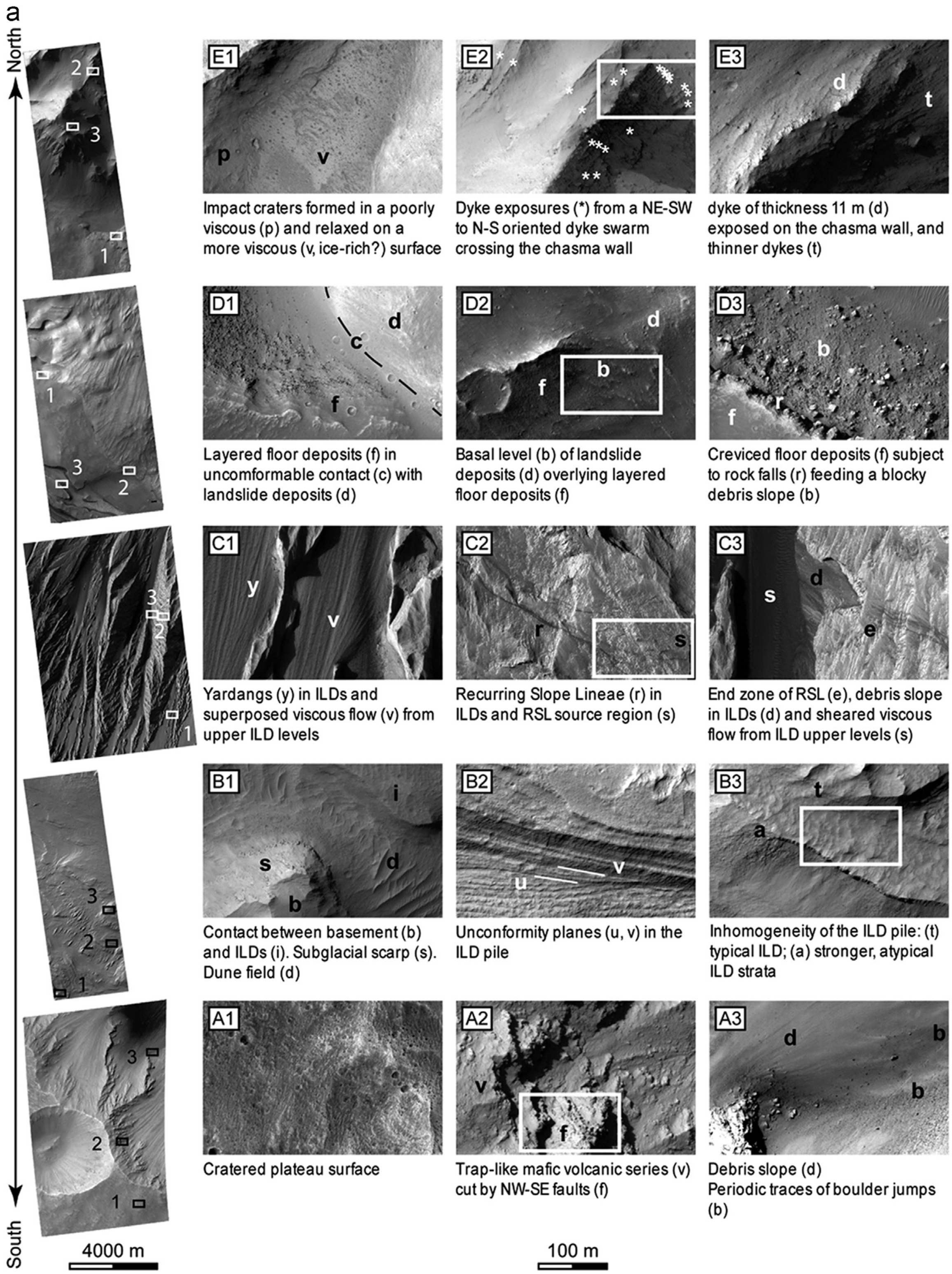

Fig. 10. (a) Examples of Valles Marineris landscapes along the cross section are presented. From bottom (South) to top (North): HiRISE image ESP_033195_1710; HiRISE image ESP_017266_1715; HiRISE image PSP_002155_1720; HiRISE image HiRISE PSP_009407_1730; HiRISE image PSP_008985_1730. ILD stands for Interior Layered Deposits. (b). Example of a hopter path in selected landscapes shown in the boxes in (a). The pixel size of image PSP_002I155_1720 (Fig. 9a, middle), initially 50 × 50 cm, is resampled to 25 × 25 cm, which is the size of pixels on the other images of Fig. 9a. The ground location of 50 hopter steps is displayed by a red surface area of 2 × 2 pixels (50 × 50 cm) and surrounded by a white halo for enhanced visibility.

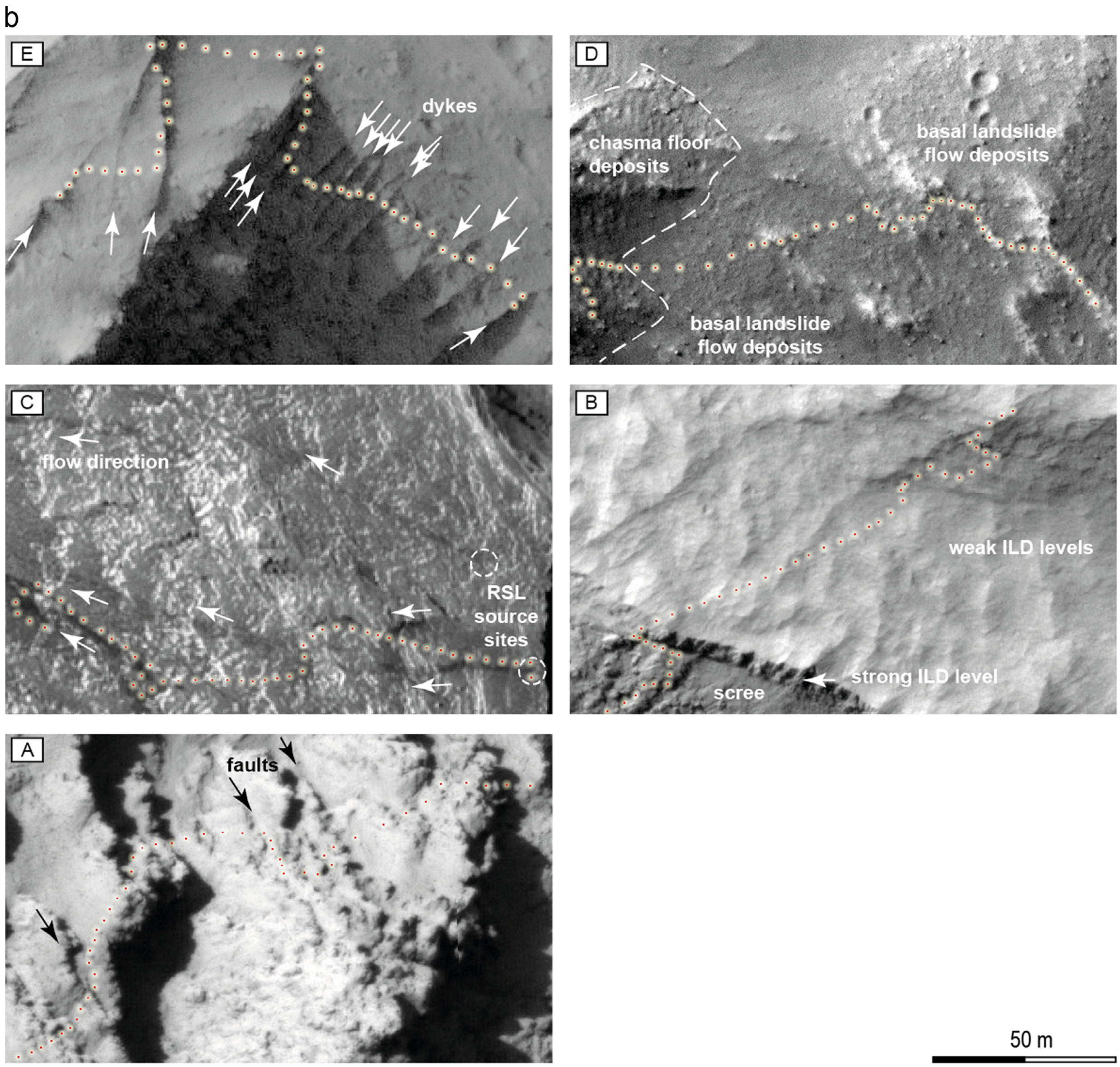

Fig. 10. (*continued*)

A 4-hopter commando could investigate the edge of the southern plateau (Fig. 10a, A1) and move downslope to the mafic volcanic pile (A2), investigating the rock magnetic properties as well as flow morphology and study flow direction indicators. Information on wallrock mineralogy [118] would be refined. Studying the faults observed to cut across the volcanic piles would be a priority science topic. Fig. 10b shows what a hopter path with 50 steps could be for investigation of these scarps (Fig. 10b, A). The debris slope below the lava pile may be interesting to study (A3); from terrestrial experience, debris slopes collects rock debris from so many sources that they provide an excellent view of the diversity of rocks upslope, including rocks having very limited exposures and could be not visible along the path followed by hopters upslope.

Two hopters could investigate the southern slope of Candor Chasma ILD mounds, starting from the contact with the basement (Fig. 10a, B1), interpreted to be a trimline [113,119]. Although usually considered to be homogeneous and parallel at large scale, the ILDs display unconformities (B2), as also identified in Aeolis Mons in Gale Crater [120] as well as variations in strength (B3) which could also be studied (Fig. 10b, B). Such changes in sedimentation conditions reflect changes in paleoenvironment conditions, some of them expressed by paleosols that hopters could clearly identify and characterise.

Two other hopters could investigate the northern ILD slopes, which present a different morphology. Yardangs are observed in the upper part of the slope (Fig. 10a, C1), gradually transforming to broad flutes northward. Hopters are especially appropriate to study RSL (C2, C3). The Valles

Marineris RSL [115], similar to others, have been described flowing from bedrock levels (e.g., [116]). In the case of Fig. 10, RSL form in ILDs. In addition to studying their composition from the field, they can access the RSL source region (C2, also Fig. 10b, C) and identify the particular geological circumstances that favour RSL development. During the summer season, the hopter cameras can monitor the source area and capture RSL initiation. In spite of recurrence, it may happen that the hopters, located right at the source area of the previous year, may need to move metres or a few tens of metres to capture the event. The RSL end zone (C3) may also be investigated, as well as the debris slopes that are frequently observed to form in the lower ILDs parts. Some of them appear to form from specific ILD levels, and may therefore be made of rock debris of composition differing from the composition of the most common ILD levels. Fig. 10a (C3) also shows the geologic processes occurring in the ILDs between the flutes. These valleys are covered by viscous flow of some material coming from the upper ILDs and covered by dunes. This viscous material displays valley-parallel banding along the flow margins, along which the dunes are deformed, denoting shearing. These features suggest that the viscous valley infilling could be made of till-covered glaciers or rock glaciers, similar to chasma glacial infilling identified by Mège and Bourgeois [119] and Gourronc et al. [113].

The floor of the chasma is frequently covered by layered sediments that are usually not considered as Interior Layered Deposits *sensu stricto*, which two hoppers could also investigate in cross section (Fig. 10a, D1) for their formation and composition. These layered floor deposits are unconformably overlain by deposits of huge chasma wall landslides, which are frequently observed in Valles Marineris (e.g., [121]) and the base level of which (D2, also Fig. 10b, D) is expected to be particularly informative to understand their mode of emplacement and the role (e.g., [122]) or absence (e.g., [123]) of lubricating fluids or ice. The layered floor deposits are sometimes fractured by huge crevices bordered by unstable scarps, the top of which is subject to rock falls that feed a fallen block mantle on the lower part of the slope (D3). The role of rock strength contrasts and fluids in rock fall triggering could be investigated.

In addition to two hopters for geology, two hopters for magnetic studies could be used to investigate the northern slope of the chasma. A hopter could study, for instance, atypical impact crater morphologies in floor deposits testifying to an unusual, perhaps ice-rich, surface material in which the topography of small impact craters relaxes (E1). A joint study of dyke swarms (E2, also Fig. 10b, E) exposed on the lower half of the chasma wall (e.g., [124] for Coprates Chasma) and the volcanic host rock would reveal magma feeding relationships based on geomorphological analysis and composition indicators, dyke flow and propagation direction (clue to magma source location), crustal magnetization properties, and variations in the orientation of the magnetic field. Dyke cross-cutting relationships (E2, E3) would inform on stress field evolution [125,126] and contribute to the understanding of the crustal geodynamics [100]. Thin dykes such as on E2 are especially

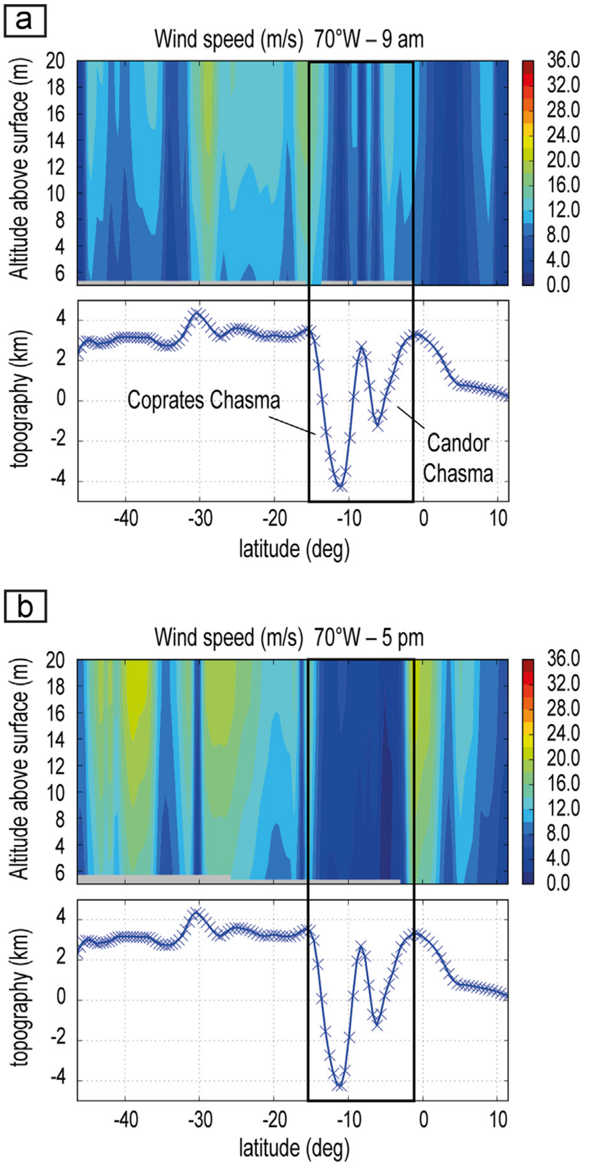

Fig. 11. High-resolution mesoscale atmospheric models in Valles Marineris [127] predict that wind speed in Candor Chasma at 70 °W is minimum at a few metres above the topographic surface at breakfast time (a, 9 a.m.) and tea time (b, 5 p.m.). Katabatic winds are maximum (30 m/s) at 10–11 p.m. and anabatic winds at 0–2 p.m. (18 m/s). The black box highlights the Valles Marineris chasmata.

informative on flow propagation direction through petrographic and structural fabric, flow indicators such as grooves and fingers, and anisotropy of magnetic susceptibility [128,129,130]; whereas thick dykes, such as E3 (thickness 10 m), record evidence of more complex emplacement history, allowing in addition to retrieve the number of magma pulses, temperature contrasts with the host rock, dyke emplacement duration, hence an estimation of the volume of fed volcanic flows, via analysis of dyke margins (e.g., [131,132,133]). Such an analysis may performed using high-resolution camera to examine the details of dyke margins, and spectrometers to identify

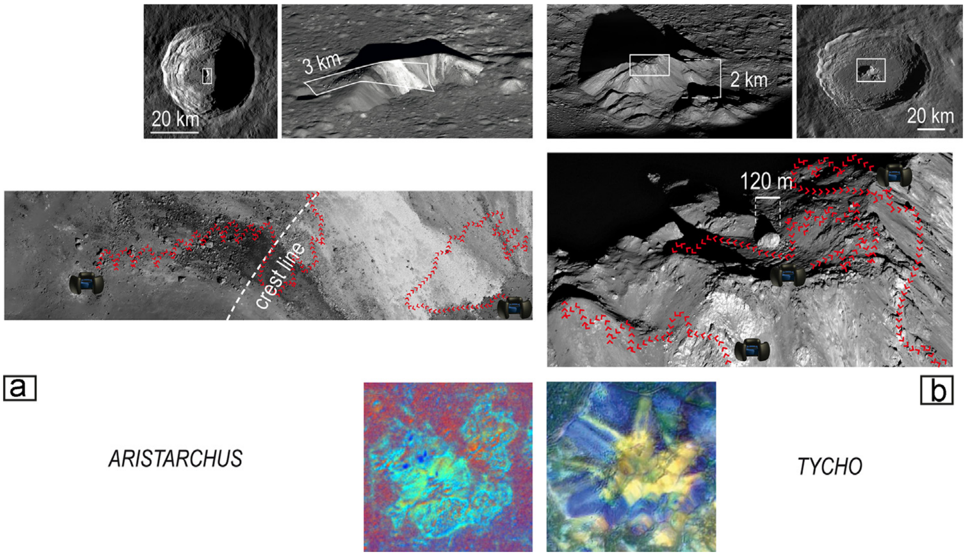

Fig. 12. Use of hopters to study lunar central peaks: Aristarchus (a) and Tycho (b), imaged by LRO/LROC. A few to several hundred jumps would be required to cover the distances indicated in red. Note the albedo variations along the Aristarchus central peak, which could indicate crustal rocks of different compositions exhumed by the impact. The top of the Tycho central peal also displays albedo variations that could indicate differences in rock composition. The 120-long boulder is located on a solidified and fractured molten rock. Variations in mineralogical assemblages at Aristarchus central peak (lower left) is illustrated by a Clementine UV/Vis colour-composite ratio image [134]. SELENE Multiband Imager colour-composite image of Tycho's central peak (lower right) emphasises almost pure anorthosite at lower elevations (blue) and up to 10% of high-Ca pyroxene (yellow) at higher elevations [135] Hopters are not to scale. (For interpretation of the references to color in this figure legend, the reader is referred to the web version of this article.)

composition variations along transects across the dykes and the host rock next to them.

Due to its high slopes, Valles Marineris is subject to strong anabatic and katabatic winds that could not only transport the hopters to an unexpected place (which may not be a negative issue). However, study sites can be selected in a way that wind velocity [127] may become negligible several metres above the surface, combining wind predictions and site geomorphology. A jumping strategy that accounts for katabatic and anabatic wind minima also minimises this risk (Fig. 11).

3.2. Moon exploration: magnetic field and central peaks

On the Moon, steep rille walls display crustal outcrops, and impact basin rims and central peaks open a window to the materials that compose the deep lunar crust. For central peak studies, the best outcrops are located on very steep slopes of young craters, such as Tycho (Fig. 12). Such steep slopes are inaccessible to rovers. Their steepness and potential instability could be a risk for static landers and in situ human investigations too. The slope of rilles are also steep, and may also be gravitationally unstable.

Because of their mechanism of formation by isostatic rebound and their widespread distribution, the crater central peaks are of critical importance for understanding the crustal structure and overall evolution of the Moon. The peaks of large craters give access to rocks excavated from deep crustal levels. For instance, high-resolution (40 cm) LRO/LROC views of the Aristarchus and Tycho (Fig. 12) indicate a high diversity of the rock outcrops that adds to the intrinsic complex tectonics of central peaks. This geological complexity is supported by the existing mineralogical interpretation of data from Clementine [134,136,137], SELENE [135], and Chandrayaan-1 [138].

On such central peaks, the much higher spectral resolution that can be obtained from in situ measurements by a hopter compared to orbital measurements would allow us to obtain much more accurate information as to the composition of the excavated rocks, hence their origin. A high resolution camera operating in the visible domain would provide accurate information as to the tectonic and geomorphologic evolution of the peak, which would be used to understand the initial stratigraphic relationships between the excavated rocks.

The hopper's ability to access rough terrain inaccessible to rovers may make them a powerful tool for geomagnetism (Fig. 13). The lunar bedrock has preserved evidence of an early dynamo generating an intense and long-lived magnetic field, the complexity of which is not yet understood. Analysis of the geometry of this magnetic field in terrains of different ages with dedicated hopters would be powerful in contributing to solve this complexity. Hypotheses regarding the nature of the magnetic source would support or discard models of double dynamos and bistable dynamo [139]. Bedrock tends to be exposed on cliff faces. A good example is the bedrock at Rima Hadley at the Apollo 15 landing site. The rocks collected during the Apollo missions were not protected from external magnetic fields after collections, and their magnetization has been overprinted. Hopters would be excellent for accessing rocks in such settings and analyse their magnetization.

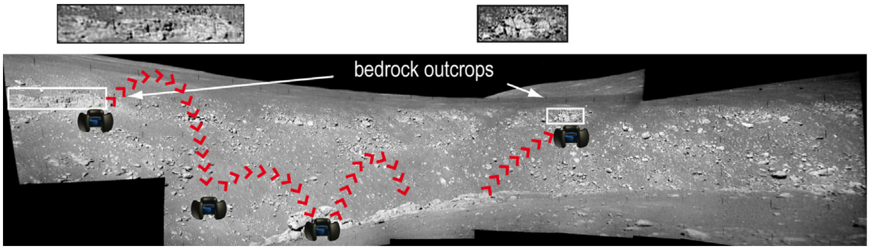

Fig. 13. Use of a hopter for studying the residual magnetization of the lunar crust at bedrock exposures at Rima Hadley, Apollo 15 site. Hopters not to scale.

3.3. Phobos exploration

On Phobos, the whole surface can be visited by hopters with a very low energy consumption. Rovers are not able to operate on such objects due to microgravity conditions and, as a result, lack of enough mass to generate the friction required between the wheels and the surface [19].

Interpretation of the blue and red terrains observed at the surface, characterisation of the internal structure of Phobos, investigation of potential resources, dust dynamics, and the future evolution of Phobos, are examples of topics that could benefit from hopter studies.

The MRO/HiRISE colour images of Phobos have revealed that the surface colour is dominated by two spectral units in the Stickney crater area, blue and red [140]. Their thickness is debated, with interpretations favouring a thin blue blanket [140] and others a mosaic of km-thick blue and red blocks [141]. These units are not yet clearly spectrally characterised, with an ongoing debate as to their possible phyllosilicate content identified by MEx/PFS, unconfirmed by MEx/OMEGA [142] but consistent with absorptions in the red and mid-infrared by MRO/CRISM [143,136]. Hopters could contribute to the understanding of the nature of the red and blue units two ways: first, the composition of these units could be accurately determined on the ground by hopters carrying near-infrared and Raman spectrometers. Secondly, whether any of the two units are a superficial blanket only, whether the blue [140] or red [141] could be determined by examining the regolith by hopter jumps in order to maximise regolith shearing by the legs and removal. The results of such hopter investigations would not only be a major step [143] toward the understanding of Phobos' regolith, which is the only source of information to constrain its composition [136], but also a major step for constraining its origin and formation processes (e.g., [144,145]) and identification of potential resources [146].

The available gravity data are currently not accurate enough for the internal structure of Phobos to reveal anomalies in the gravity field [147]. Data from the MaRS radiometer experiment of Mars Express indicates, however, that Phobos has a high porosity, estimated to ca. 30% [144], and could contain large voids or an abundance of low density material such as water ice [148]. Phobos control point tracking has revealed a libration amplitude that favours an overall homogeneous Phobos interior [149], especially consistent with the presence of water ice. A gravity three-dimensional experiment ("Phobos is evidently the most interesting application of 'triaxial geophysics'"; [150]) carried by a hopter network (Fig. 7) would be able to provide a detailed view of the gravity anomalies at the scale the network would be deployed, from shallow and small-scale to deep and large-scale. Additional information as to the distribution of masses in Phobos' interior could be provided by hopter acquisition of two-way Doppler measurements in X-band between hopters and Earth-ground stations and implementation of star-tracking techniques [151]; nevertheless, implementation of such an experiment would require direct and long-lasting radio communications between hopters and the Earth, which needs a detailed feasibility study.

The distribution of masses within Phobos, a direct consequence of its accretion history [144,145] constrains the future evolution of Phobos, which will be disrupted before it would crash on Mars due to tidal forces. A seismic survey [150] conducted by a hopter network (Fig. 7) would determine the Lamé coefficients, which define the elastic properties of Phobos, and help predict its disruption at the Roche limit, estimated to occur in the next tens of million years [152,153], with the first observable effects starting perhaps as soon as in a few thousand years [154]. In addition to these parameters, which can be used to refine Phobos disruption models, the study of relative hopter displacement in a hopter network used as a geodetic network, using laser ranging for instance, would provide direct and continuous measurements of the current tidal effects. These would constrain the Phobos evolution models further, and help determine the timing of future disruption.

Models predict that solar radiations and wind plasma flow at the surface of Phobos may cause dust production near the surface of Phobos, resulting in dust trails and a dust ring in its orbit (e.g., [155]). The attempts at identifying such dust concentrations from various datasets (see [155]), until the MEx/HRSC dataset [142], have failed. These particles are below the level of detection of the current sensors, placing an upper limit to dust particle size and abundance. Flashing LEDs mounted next to hopter cameras (see Section 2.5) would help identify and characterize dust particle on the very near surface of Phobos, and track their motion [45].

3.4. Asteroid resources

Hopters can also be used to identify and characterise resources, in addition to answering basic science questions. Many asteroids are thought to have abundant resources in metals ("… practically a whole asteroid may be considered as a deposit of metals"; [156]), with attention particularly drawn on metals from the Platinum group [157]. Among others, of exceptional interest is asteroid 16 Psyche, which appears to be fully composed of unoxidised metals [158,159], analogue in composition and maybe in significance to a planetary core as well as a possible parent body of mesosiderites [160,161]. Although the economic viability of asteroids exploration remains questionable on the short to middle term, their exploration for resources has attracted a growing interest over the last decade with the idea that combining science and profit will be beneficial to all [162]. The investigations of the REXIS (Regolith X-ray Imaging Spectrometer) instrument of the OSIRIS-Rex mission, planned for exploration of asteroid 101955 Bennu with launch in 2016, may be considered as the first step toward detailed asteroid resource investigations.

Because of the difficulties of moving at the surface of such low-gravity bodies as asteroids, as well as tumbling issues, mining companies such as Deep Space Industries and Planetary Resources envisage In situ prospection of asteroids using CubeSats. Hopters would provide low cost mobile alternatives, and instrumentation as on Fig. 7 would provide the necessary tools for resource evaluation site by site. Due to their mobility, the number of required hopters to study the surface of asteroids would be much smaller than the number of CubeSats, and guarantee access to the whole asteroid surface.

3.5. Exploration of other low-gravity bodies

Exploring further objects, such as cometary nuclei, KBOs, trojans and others, is also thought to be possible using hopters, however with additional constraints for bodies undergoing very low insolation, making impossible battery refill using solar energy using the technology existing today. Nevertheless, this problem may be mitigated with more mass devoted to battery on kbopters than on other hopter categories at the expense of the payload. This would not harm the scientific interest of a mission because many instruments, including cameras, spectrometers and others, are not much weight demanding, and because the number of instruments onboard each hopters can be decreased by increasing the number of hopters. Scientific objective may be related to the interpretation of icy landscapes on giant planets' satellites, extended to analysis of surface material loss by cometary nuclei similar to the analysis that was mentioned for investigating Phobos dust.

4. Concluding remarks

The advantages of using the hopter platform compared to rovers and other hopping platforms include (1) concept simplicity, which increases reliability and robustness; (2) ability at implementing a variety of displacement strategies, including networking, opening the possibility of undertaking three-dimensional geological and geophysical surveys; (3) versatility: hopters may be considered as main mission platforms, secondary platforms connected to a lander or rover for exploring risky terrain, or a help to human in situ exploration in areas where the scientific reward is worth the potential loss of a hopter but not a human being; (4) high manoeuvrability: the symmetric distribution of the three actuating legs determines the jumping direction by adjusting jump energy in each arm separately. Hopters are also symmetric (no top, no bottom), which in case of unpredicted jump target behaviour, ensures mobility recovery; (5) extreme mobility: jumping high is made possible by the low mass and small size. Obstacles as high as 1.5 m on Earth, 4 m on Mars, and 9 m on the Moon can be overcome, which in most circumstances (e.g., very high cliffs devoid of benches) on Mars and the Moon is enough to travel far in mountains and other areas with steep slopes or large boulders. Much higher cliffs can be crossed if $\sim 1 \times 1$ m benches divide the cliff into sections having subvertical walls lower than these values. The small weight allows to consider crossing terrains that would be too loose for much heavier rovers. Several kilometres can be travelled without battery recharge; (6) new balance between risk and scientific benefit: in a several hopter mission, scientists and engineers may decide that a site of exceptional scientific interest but presenting a risk of platform damage may be worth taking the risk to visit, given the cost of the platform and the number of other hopters still in operation; (7) launched mass cost: for instance, a hopter platform and its payload is 90 times less expensive than Curiosity. Undoubtedly, the number of scientific instruments onboard a hopter is less than the number of instruments that can be placed on a rover, and there is no way to attain the level of robotic sophistication that can be attained in Curiosity. Nevertheless, if the same costs are considered, the opportunity of having tens of hopters at the surface of Mars opens an avenue to scientific objectives that geologists and geophysicists would dream to attain on other solid bodies, based on their scientific experience on Earth, and are unachievable with other types of platforms.

The considerable improvement expected in scientific understanding by exploring other Solar System bodies using hopters also justifies that efforts are directed towards dramatic instrument miniaturisation to fit the mass constraints. All the instruments mentioned in this work either exist at a level of technological development that is consistent with the mass constraints for hopper integration, or are thought to be miniaturised enough after a couple of years of development. Joint integration of the main system and the instrument subsystems is an especially promising direction for even higher platform and instrument mass gain. Microtechnology and MEMS technology, by itself, can only meet this challenge in part, however. Without joint integration of the vehicle system and the instrument subsystems, little is gained, since the interfacing and packaging otherwise necessary, or at least used, for the MEMS devices will multiply their mass by several orders of magnitude. Best leverage is achieved if the bulk and surfaces of the carriers for the components and their connections (MEMS, electronics and circuitry) are used for additional tasks, for instance carrying load as members of the chassis, or being the carrier of thin or thick film components like solar cells or active coatings for thermal management. Judging from vehicles with similar or worse mass limitations, like the above mentioned nanosatellite and spherical rover, an extremely competent hopper with the stated mass, is within reach.

Acknowledgements

This work was conducted with financial help from the Foundation for Polish Science (TEAM/2011-7/9), the Atlab project (REGPOT-2011-1 EU FP7) and ING PAN. Antoine Lucas kindly generated the digital elevation model used in Fig. 9, Aymeric Spiga produced Fig. 12 from Spiga and Forget (2009)'s atmospheric model. Per Samuelsson is thanked for authorisation of using the SMIPS image reproduced on Fig. 2. The paper benefitted from discussions with many colleagues, including Hans Rickman, Tony Cook, Jérôme Dyment, Maria Gritsevich, Ernst Hauber, Akos Kereszturi, Tomasz Kuciński, Benoit Langlais, Antoine Mocquet, Jürgen Oberst, Jouni Peltoniemi, Bernard Schmitt, and others.

References

[1] W.B. Banerdt, S. Smrekar, L. Alkalai, T. Hoffman, R. Warwick, K. Hurst, W. Folkner, P. Lognonné, T. Spohn, S. Asmar, D. Banfield, L. Boschi, U. Christensen, V. Dehant, D. Giardini, W. Goetz, M. Golombek, M. Grott, T. Hudson, C. Johnson, G. Kargl, N. Kobayashi, J. Maki, D. Mimoun, A. Mocquet, P. Morgan, M. Panning, W.T. Pike, J. Tromp, T. can Zoest, R. Weber, M. Wieczorek and the InSight Team, Insight: an integrated exploration of the interior of Mars, in: 43rd Lunar and Planetary Science Conference, Abstract 2838, 2012.

[2] V. Dehant, B. Banerdt, P. Lognonné, M. Grott, S. Asmar, J. Biele, D. Breuer, F. Forget, R. Jaumann, C. Johnson, M. Knapmeyer, B. Langlais, M. LeFeuvre, D. Mimoun, A. Mocquet, P. Read, A. Rivoldini, O. Romberg, G. Schulbert, S. Smrekar, T. Spohn, P. Tortora, S. Ulamec, S. Vennerstrøm, Future Mars geophysical observatories for understanding its internal structure, rotation, and evolution, Planet. Space Sci. 68 (2012) 123–145.

[3] T. Spohn, K. Seiferlin, A. Hagermann, J. Knollenberg, A.J. Ball, M. Banaszkiewicz, J. Benkhoff, S. Gadomski, W. Gregorczyk, J. Grygorczuk, M. Hlond, G. Kargl, E. Kührt, N. Kömle, J. Krasowski, W. Marczewski, J.C. Zarnecki, MUPUS – a thermal and mechanical properties probe for the Rosetta lander Philae, Space Sci. Rev. 128 (2007) 339–362.

[4] C. Holstein-Rathlou, H.P. Gunnlaugsson, J.P. Merrison, K.M. Bean, B. A. Cantor, J.A. Davis, R. Davy, N.B. Drake, M.D. Ellehoj, W. Goetz, S. F. Hviid, C.F. Lange, S.E. Larsen, M.T. Lemmon, M.B. Madsen, M. Malin, J.E. Moores, P. Nørnberg, P. Smith, L.K. Tamppari, P. A. Taylor, Winds at the Phoenix landing site, J. Geophys. Res. 115 (2010) EE00E18, http://dx.doi.org/10.1029/2009JE003411.

[5] J.A. Whiteway, L. Komguem, C. Dickinson, C. Cook, M. Illnicki, J. Seabrook, V. Popovici, T.J. Duck, R. Davy, P.A. Taylor, J. Pathak, D. Fisher, A.I. Carswell, M. Daly, V. Hipkin, A.P. Zent, M.H. Hecht, S. E. Wood, L.K. Tamppari, N. Renno, J.E. Moores, M.T. Lemmon, F. Daerden, P.H. Smith, Mars water-ice clouds and precipitation, Science 325 (2009) 68–70.

[6] M.P. Golombek, J. Grant, D. Kipp, A. Vasavada, R. Kirk, R. Fergason, P. Bellutta, F. Calef, K. Larsen, Y. Katayama, A. Hurtas, R. Beyer, A. Chen, T. Parker, B. Pollard, S. Lee, Y. Sun, R. Hoover, H. Sladek, J. Grotzinger, R. Welch, E. Noe Dobrea, J. Michalski, M. Watkins, Selection of the Mars Science Laboratory landing site, Space Sci. Rev. 170 (2012) 641–737, http://dx.doi.org/10.1007/s11214-012-9916-y.

[7] A. Kereszturi, Geologic field work on Mars: distance and time issues during surface exploration, Acta Astronaut. 68 (2011) 1686–1701.

[8] NASA, Mars Science Laboratory Press Release, 08/07/2014, 〈http://mars.jpl.nasa.gov/msl/news/whatsnew/index.cfm?FuseAction=ShowNews&NewsID=1665〉, 2014a (consulted February 4th, 2015).

[9] E. Lakdawalla, Mars Society blog, 19/08/2014, 〈http://www.planetary.org/blogs/emily-lakdawalla/〉, 2014 (consulted February 4th, 2015).

[10] NASA, Mars Science Laboratory Press Release, 11/09/2014, 〈http://mars.jpl.nasa.gov/msl/news/whatsnew/index.cfm?FuseAction=ShowNews&NewsID=1705〉, 2014b (consulted February 4th, 2015).

[11] C. White, D. Limonadi, C. Collins, G. Antoun, C. Roumeliotis, L. Jandura, B. Hallet, J. Melko, M. Robinson, R. Sletten, Keeping the MSL rover safe against slip and settling while sampling, in: Proceedings of the 2014 IEEE Aerospace Conference, 2014, pp.?1–9, 10.1109/AERO.2014.6836407.

[12] ESA, Press Release, 8?November 2014, 〈http://sci.esa.int/jump.cfm?oid=54468〉 (consulted February 4th, 2015).

[13] A. Ellery, Robot–environment interaction – the basis for mobility in planetary microrovers, Robot. Auton. Syst. 51 (2005) 29–39.

[14] E. Argand, Sur l'arc des Alpes occidentales, Eclogae Geol. Helv. 14 (1916) 145–192.

[15] M.M. Gunther, H. Ishida, H. Kumakura, Y. Nakano, The jump as a fast mode of locomotion in arboreal and terrestrial biotopes, Z. Morph. Anthr. 78 (1991) 341–372.

[16] P. Fiorini, M. Marchesi, Robustness concepts for hopping robots, In Proc. 8th ESA Workshop on Avanced Space Technologies for Robotics and Automation (2004) p.8.

[17] S. Ulamec, V. Kuruchenko, J. Biele, A. Bogatchev, A. Makurin, S. Matrossov, Hopper concepts for small body landers, Adv. Space Res. 47 (2011) 428–439.

[18] A.L. Kermudzhian, A.F. Bogomolov, P.N. Brodskii, V.V. Gromov, Sh. Sh. Dolginov, F.F. Kirnozov, G.V. Kozlov, V.I. Komissarov, L.V. Ksanfomality, V.I. Kucherenko, B.N. Martynov, V.K. Mishkinyuk, A.V. Mitskevich, G.N. Rogovskii, P.S. Sologub, Yu.A. Surkov, A.V. Turobinskii, Study of Phobos´ Surface with amovable Robot, in: Proceedings of the International Workshop: Phobos-Scientific and Methodological Aspects of the Phobos Study, USSR Academy of Sciences, Moscow, 1988, pp.?357–367, (original in Russian).

[19] L. Richter, Principles for robotic mobility on minor solar system bodies, Robot. Auton. Syst. 23 (1998) 117–124.

[20] T. Yoshimitsu, T. Kubota, I. Nakatani, MINERVA rover which became a small artificial solar satellite, in: Proceedings of the 20th Annual AIAA/USU Conference Small Satellites, SSC06-IV-4, 2005.

[21] C. Dietze, F. Herrmann, S. Kuß, C. Lange, M. Scharringhausen, L. Witte, T. van Zoest, H. Yano, Landing and mobility concept for the small asteroid lander mascot on asteroid 1999 JU3, in: Proceedings of the 61st International Astronautical Congress, Prague, IAC-10. A3.5.8, 2010, p.13.

[22] R.G. Reid, L. Roveda, I.A.D. Nesnas, M. Pavone, Contact dynamics of internally-actuated platforms for the exploration of small Solar System bodies, in: Proceedings of the 12th International Symposium on Artificial Intelligence, Robotics and Automation in Space (i-SAIRAS2014), Saint-Hubert, Canada, p.9.

[23] B.C. Clark, Compet Hopper: a mission concept for exploring the heterogeneity of comets, Asteroids, Comets, Meteors, LPI Contribution 1405, abstract 8131, 2008.

[24] S.D. Howe, R.C. O'Brien, R.M. Ambrosi, B. Gross, J. Katalenich, L. Sailer, M. McKay, J.C. Bridges, N.P. Bannister, The Mars Hopper: an impulse driven, long range, long-lived mobile platform utilizing in-situ Martian resources, Acta Astronaut. 69 (2011) 1050–1056.

[25] E. Shafirovich, M. Salomon, I. Gökalp, Mars hopper versus Mars rover, Acta Astronaut. 59 (2006) 710–716.

[26] H.R. Williams, J.C. Bridges, R.M. Ambrosia, M.-C. Perkinson, J. Reed, L. Peacocke, N.P. Bannister, S.D. Howec, R.C. O'Brien, A.C. Klein, Mars reconnaissance lander: vehicle and mission design, Planet. Space Sci. 59 (2011) 1621–1631.

[27] G. Landis, D. Linne, Mars exploration with a self-refueling hopper, Concepts and Approaches For Mars Exploration, Lunar and Planetary Institute, Houston, Texas, Abstract 6098, p. 187.

[28] P. Fiorini, F. Bovo, L. Bertelli, Solving the landing problem of hopping robots: the elastic cage design, in: Proceedings of the ASTRA 2008 S05-04, ESTEC Noordwijk, The Netherlands, 2008, p. 8.

[29] S. Montminy, E. Dupuis, H. Champliaud, Mechanical design of a hopper robot for planetary exploration using SMA as a unique source of power, Acta Astron. 62 (2008) 438–452.

[30] F.C. Bruhn, H. Kratz, J. Warell, C.-I. Lagerkvist, V. Kaznov, J.A. Jones, L. Stenmark, A preliminary design for a spherical inflatable microrover for planetary exploration, Acta Astronaut. 63 (2008) 618–631.

[31] J.C. Castillo-Rogez, M. Pavone, J.A. Hoffman, I.A.D. Nesnas, Expected Science Return of Spatially-Extended In-Situ Exploration at Small Solar System Bodies, in: Proceedings of the Aerospace Conference,

2012 IEEE, 2012, pp.1–15, http://dx.doi.org/10.1109/AERO.2012.6187034.
[32] M. Lange, C. Hühne, O. Mierheim, A. Braukhane, T.-M. Ho, C. Lange, S. Wagenbach, L. Witte, MASCOT – a lightweight multi-purpose lander platform, in: Proceedings of the European conference on spacecraft structures, materials and environmental testing 2012, ESTEC Noordwijk, The Netherlands, 2012, p. 4.
[33] J. Gurgurewicz, D. Mège, J. Grygorczuk, H. Rickman, L. Wisniewski, The Highland Terrain Hopper: a new locomotion system for exploration of Mars and other low-gravity planetary bodies, in: Proceedings of the 40th COSPAR Scientific Assembly, B0.2-0043-14, 2014.
[34] D. Mège, J. Gurgurewicz, J. Grygorczuk, L. Wisniewski, H. Rickman, Exploring Martian mountains with Galago, the highland terrain hopper, in: Proceedings of the 8th International Conference on Mars, Pasadena, Abstract 1251, 2014.
[35] L. Wisniewski, J. Grygorczuk, D. Mège, J. Gurgurewicz, T. Kucinski, T. Barcinski, H. Rickman, A. Nicolau-Kuklinska, Planetary Highland Hopper, in: Proceedings of the Third workshop on penetrometry in the Solar System, Seggau Castle, Austria, May 19–21, 2014.
[36] F. Bruhn, J. Köhler, L. Stenmark, NanoSpace-1: the Impacts of the first Swedish nanosatellite on spacecraft architecture and design, Acta Astronaut. 53 (2003) 633–643.
[37] H. Nguyen, R. Thorslund, G. Thornell, J. Köhler, L. Stenmark, Structural integrity of flat silicon panels for nanosatellites – modeling and testing, J. Spacecr. Rocket 43 (2006) 1319–1327.
[38] H. Kratz, M. Karlsson, A. Eriksson, J. Köhler, L. Stenmark, G. Thornell, Design and modeling of a thermally regulated communications module for nanospacecraft, J. Spacecr. Rockets 43 (2006) 1377–1386.
[39] O. Brown, P. Eremenko, Fractionated space architectures: a vision for responsive space, in: Proceedings of the 4th Responsive Space Conference, Los Angeles, California, RS4-2006-1002, 2006, p.13.
[40] B.J. Bozlee, A.K. Misra, S.K. Sharma, M. Ingram, Remote Raman and fluorescence studies of mineral samples, Spetrochim. Acta Part A 61 (2005) 2342–2348.
[41] H.D. Smith, C.P. McKay, A.G. Duncan, R.C. Sims, A.J. Anderson, P. R. Grossl, An instrument design for non-contact detection of biomolecules and minerals on Mars using fluorescence, J. Biol. Eng. 8 (2014) 16.
[42] M.C. Storrie-Lombardi, B. Sattler, Laser-induced fluorescence emission (L.I.F.E.): *In?situ* nondestructive detection of microbial life in the ice covers of Antarctic lakes, Astrobiology 9 (2009) 659–672, http://dx.doi.org/10.1089/ast.2009.0351.
[43] P. Rochette, J. Gattacceca, M. Menvielle, P. Eisenlohr, V. Chevrier, Interest and design of magnetic properties measurements on planetary and asteroidal landers, Planet. Space Sci. 52 (2004) 987–995.
[44] B. Allen, J. Grindlay, J. Hong, R.P. Binzel, R. Masterson, N.K. Inamdar, M. Chodas, M.W. Smith, M.W. Bautz, S.E. Kissel, J. Villasenor, M. Oprescu, N. Induni, The REgolith X-Ray Imaging Spectrometer (REXIS) for OSIRIS-Rex: Identifying regional elemental enrichment on asteroids, in: Proceedings of the SPIE 2013 Conference on Optical Modeling and Performance Predictions VI, San Diego, CA, USA, 2013, arXiv:1309.6665 [astro-ph.IM], http://dx.doi.org/10.1117/12.2041715〉.
[45] A.C. Cook, A.J. Higgs, R.A. Pocock, Close range remote sensing of levitated dust particles, in: Proceedings of the European Planetary Science Congress 2014, EPSC Abstracts 9, EPSC2014-817, 2014.
[46] N. Kishida, M. Shinji, T. Tsutsui, A. Hirama, Densitometry for sprayed concrete floating dust tunnel construction by digital camera, in: Proceedings of the ITA-AITES World Tunnel Congress Budapest, P-?07-03, 2009.
[47] C. Roussel, J. Verdun, J. Cali, M. Maia, J.-F. D'Eu, GRAVIMOB, a new gravimetry and gradiometry mobile system for the subsea domain, in: Proceedings of the G2 Colloquium 17–19 November 2014, Strasbourg, France, 2014.
[48] A. Persson, G. Thornell, H. Nguyen, Radiation tolerance of a spin-dependent tunneling magnetometer for space applications, Meas. Sci. Technol. 22 (2011) 045204, http://dx.doi.org/10.1088/0957-0233/22/4/045204.
[49] A. Persson, R.S. Bejhed, H. Nguyen, K. Gunnarsson, B.T. Dalslet, F. W. Østerberg, M.F. Hansen, P. Svedlindh, Low-frequency noise in planar hall effect bridge sensors, Sens. Actuators A: Phys. 171 (2011) 212–218.
[50] T. Kuwahara, Y. Yoshida, Y. Tomioka, K. Fukuda, M. Fukuyama, Y. Shibuya, International scientific micro-satellite RISESAT based on Space Plug and Play Avionics, in: Proceedings of the 26th Annual AIAA/USU Conference Small Satellites, SSC12-I-1.
[51] C. Honsho, J. Dyment, K. Tamaki, M. Ravilly, H. Horen, P. Gente, Magnetic structure of a slow spreading ridge segment: insights from near-bottom magnetic measurements on board a submersible, J. Geophys. Res. 114 (2009) B05101, http://dx.doi.org/10.1029/2008JB005915.
[52] Y. Nakamura, G.V. Latham, H.J. Dorman, J.E. Harris, Passive seismic experiment long period event catalog, 1969 Day 202-1977 Day 273, ALSEP Stations 11, 12, 13, 14, 15, and 16 UTIG Tech. Rep. 18, 1981, revised January 2004.
[53] D.L. Anderson, W.F. Miller, G.V. Latham, Y. Nakamura, M.N. Toksöz, A.M. Dainty, F.K. Duennebier, A.R. Lazarewicz, R.L. Kovach, T.C. D. Knight, Seismology on Mars, J. Geophys. Res. 82 (1977) 4524–4546.
[54] W.B. Banerdt, S. Smrekar, K. Hurst, P. Lognonné, T. Spohn, S. Asmar, D. Banfield, L. Boschi, U. Christensen, V. Dehant, W. Folkner, D. Giardini, W. Goetz, M. Golombek, M. Grott, T. Hudson, C. Johnson, G. Kargl, N. Kobayashi, J. Maki, D. Mimoun, A. Mocquet, P. Morgan, M. Panning, W.T. Pike, J. Tromp, T. van Zoest, R. Weber, M. Wieczorek and the InSight Team, Insight: a Discovery mission to eplore the interior of Mars, in: Proceedings of the 44th Lunar Planetary Science Conference, Abstract 1915, 2013.
[55] P. Lognonné, W.B. Banerdt, K. Hurst, D. Mimoun, R. Garcia, M. Lefeuvre, J. Gagnepain-Beyneix, M. Wieczorek, A. Mocquet, M. Panning, E. Beucler, S. Deraucourt, D. Giardini, L. Boschi, U. Christensen, W. Goetz, T. Pike, C. Johnson, InSight and single-station broadband seismology: from signal and noise to interior structure determination, in: Proceedings of the 43rd Lunar Planetary Science Conference, Houston, Texas, Abstract 1983, 2012.
[56] P.-A. Dandonneau, P. Lognonné, W.B. Banerdt, S. Deraucourt, T. Gabsi, J. Gagnepain-Beyneix, T. Nébut, O. Robert, S. Tillier, K. Hurst, D. Mimoun, U. Christensen, M. Bierwirth, R. Roll, T. Pike, S. Calcutt, D. Giardini, D. Mance, P. Zweifel, P. Laudet, L. Kerjean, R. Perez and the SEIS Team. The SEIS InSight VBB Experiment, 44th Lunar Planet. Sci. Conf., Abstract 2006, 2013.
[57] N.E. Bowles, W.T. Pike, N. Teanby, G. Roberts, S.B. Calcutt, J. Hurley, P. Coe, J. Wookey, P. Dunton, I. Standley, J. Temple, R. Irshad, J. Taylor, T. Warren, C. Charalambous, Performance and noise modelling of the short period seismometer SEIS-SP, part of the SEIS instrument for NASA's 2016 InSight Mission, in: 46th Lunar and Planetary Science Conference, Houston, Texas, Abstract 2146, 2015.
[58] S. Kumar, Design and fabrication of micromachined silicon suspensions (PhD thesis), Imperial College, London, 2007, 311.
[59] M.P. Panning, E. Beucler, M. Drilleau, A. Mocquet, P. Lognonné, B. Banerdt, Verifying single-station seismic approaches using Earth-based data: preparation for data return from the InSight mission to Mars, Icarus 248 (2015) 230–242.
[60] N.A. Teanby, Predicted detection rates of regional-scale meteorite impacts on Mars with the InSight short-period seismometer, Icarus 256 (2015) 49–62.
[61] G.G. Sorrells, A preliminary investigation into the relationship between long-period seismic noise and local fluctuations in the atmospheric pressure field, Geophys. J. R. Astron. Soc. 26 (1971) 71–82.
[62] H. Steffen, The importance of instrument location on barometric pressure-induced noise, Bull. Inf. Marées Terr. 141 (2005) 11 293–11 302.
[63] W. Zürn, J. Exß, H. Steffen, C. Kroner, T. Jahr, M. Westerhaus, On reduction of long-period horizontal seismic noise using local barometric pressure, Geophys. J. Int. 171 (2007) 780–796.
[64] N.A. Teanby, J. Wookey, Seismic detection of meteorite impacts on Mars, Phys. Earth Planet. Int. 186 (2011) 70–80.
[65] R.J. Phillips, Expected Rates of Marsquakes, Lunar and Planetary Institute, Technical Reports 91-02, 1991, pp.?35 38.
[66] D.R. Lammlein, G.V. Latham, J. Dorman, Y. Nakamura, M. Ewing, Lunar seismicity, structure, and tectonics, Rev. Geophys. Space Phys. 12 (1974) 1–21.
[67] G. Neukum, R. Jaumann, H. Hoffmann, E. Hauber, J.W. Head, A. T. Basilevsky, B.A. Ivanov, S.C. Werner, S. van Gasselt, J.B. Murray, T. McCord, the HRSC Co-Investigator TEAM, Recent and episodic volcanic and glacial activity on Mars revealed by the high resolution stereo camera, Nature 432 (2004) 971–979.
[68] M. Knapmeyer, J. Oberst, E. Hauber, M. Wählisch, C. Deuchler, R. Wagner, Working models for spatial distribution and level of Mars' seismicity, J. Geophys. Res. 111 (2006) E11006, http://dx.doi.org/10.1029/2006JE002708.
[69] P. Lognonné, Planetary seismology, Annu. Rev. Planet. Sci. 33 (2005) 571–604.
[70] R. Weber, P.-Y. Lin, E. Garnero, Q. Williams, P. Lognonné, Seismic detection of the lunar core, Science 331 (2011) 309–312.

[71] S.R. McNutt, Volcanic seismology, Annu. Rev. Earth Planet. Sci. 32 (2005) 461–491.
[72] J. Deparis, D. Jongmans, F. Cotton, L. Baillet, F. Thouvenot, D. Hantz, Analysis of rock-fall and rock-fall avalanche seismograms in the French Alps, Bull. Seismol. Soc. Am. 98 (2008) 1781–1796.
[73] C. Hibert, A. Mangeney, G. Grandjean, N.M. Shapiro, Slope instabilities in Dolomieu crater, Réunion Island: from seismic signals to rockfall characteristics, J. Geophys. Res. 116 (2011) F04032, http://dx.doi.org/10.1029/2011FJ002038.
[74] J. Zhao, L. Moretti, A. Mangeney, E. Stutzmann, H. Kanamori, Y. Capdeville, E.S. Calder, C. Hibert, P.J. Smith, P. Cole, A. LeFriant, Model space exploration for determining landslide source history from long-period seismic data, Pure Appl. Geophys. 172 (2015) 389–413, http://dx.doi.org/10.1007/s00024-014-0852-5.
[75] L. Moretti, A. Mangeney, Y. Capdeville, E. Stutzmann, C. Huggel, D. Schneider, F. Bouchut, Numerical modeling of the Mount Steller landslide flow history and of the generated long period seismic waves, Geophys. Res. Lett. 39 (2012) L16402, http://dx.doi.org/10.1029/2012GL052511.
[76] M. Nettles, G. Ekström, Glacial earthquakes in Greenland and Antarctica, Annu. Rev. Earth Planet. Sci. 38 (2010) 467–491.
[77] F. Walter, J.M. Amundson, S. O'Neel, M. Truffer, M. Fahnestock, H. A. Fricker, Analysis of low-frequency seismic signals generated during a multiple-iceberg calving event at Jakobshavn Isbrae, Greenland, J. Geophys. Res. 117 (2012) F01036, http://dx.doi.org/10.1029/2011JF002132.
[78] S. Danesi, S. Bannister, A. Morelli, Repeating earthquakes from rupture of an asperity under an Antarctic outlet glacier, Earth Planet. Sci. Lett. 253 (2007) 151–158.
[79] K.L. Tanaka, J.A. Skinner, Jr., J.M. Dohm, R.P. Irwin, III, E.J. Kolb, C.M. Fortezzo, T. Platz, G.G. Michael, T.M. Hare, Geologic Map of Mars, U. S. Geological Survey Scientific Investigations Map 3292, scale 1:20,000,000, pamphlet, p. 43, 〈http://dx.doi.org/10.3133/sim3292〉.
[80] U.K. Petersen, M.S. Andersen, R.S. White, SeiFaBa Group, Seismic imaging of basalts at Glyvursnes, Faroe Islands: hunting for future exploration methods in basalt covered areas, First Break, 24, , 2006, 45–52.
[81] A. Ziolkowski, P. Hanssen, R. Gatliff, H. Jakubowicz, A. Dobson, G. Hampson, X.-Y. Li, E. Liu, Geophys. Prospect. 51 (2003) 169–182.
[82] D. Colombo, T. Keho, G. McNeice, Integrated seismic-electromagnetic workflow for sub-basalt exploration in northwest Saudi Arabia, Lead. Edge 31 (2012) 42–52, http://dx.doi.org/10.1190/1.3679327.
[83] T. Aizawa, T. Kimura, T. Matsuoka, T. Takeda, Y. Asano, Application of MEMS accelerometer to geophysics, Int. J. Jpn. Comm. Rock Mech. 4 (2008) 1–4.
[84] M. Farine, N. Thorburn, D. Mougenot, General application of MEMS sensors for land seismic acquisition, is it time? Lead. Edge 23 (2004) 246–250.
[85] M.S. Hons, R.R. Stewart, D.C. Lawton, M.B. Bertram, G. Hauer, Field data comparisons of MEMS accelerometers and analog geophones, Lead. Edge 27 (2008) 896–903, http://dx.doi.org/10.1190/1.2954030.
[86] D. Mougenot, Thorburn, MEMS-based accelerometers for land seismic acquisition: is it time? Lead. Edge 23 (2004) 246–250, http://dx.doi.org/10.1190/1.1690897.
[87] D. Mougenot, A. Cherepovskiy, L. JunJie, MEMS-based accelerometers: expectations and practical achievements, First Break 29 (2011) 85–90.
[88] J. Lainé, D. Mougenot, A high-sensitivity MEMS-based accelerometer, Lead. Edge 33 (2014) 1234–1242, http://dx.doi.org/10.1190/tle33111234.1.
[89] D. Mougenot, Pushing toward the low frequencies, World Oil 226 (9) (2005) 25–30.
[90] F. Mailly, A. Giani, A. Martinez, R. Bonnot, P. Temple-Boyer, A. Boyer, Micromachined thermal accelerometer, Sens. Actuators A 103 (2003) 359–363.
[91] J. Meunier, J.-P. Ménard, Seismic noise without a seismic source, in: Proceedings of the EAGE 66th Conference on Exhibition, H022, 2004, p. 4.
[92] S. Bonnefoy-Claudet, F. Cottno, P.-Y. Bard, The nature of noise wavefield and its applications for site effect studies, a literature review, Earth-Sci. Rev. 75 (2006) 205–227.
[93] D. Mougenot, Land broadband seismic from the receiver perspective, in: Proceedings of the EAGE 66th Conference on Exhibition, I04, 2013,10.3997/2214-4609.20131232.
[94] S. Falsaperla, M. Neri, Seismic footprints of shallow dyke propagation at Etna, Italy, Sci. Rep. 5 (2015) 11908.
[95] C.M. Weitz, T.J. Parker, M.H. Bulmer, F.S. Anderson, J.A. Grant, Geology of Melas Chasma landing site for the Mars Exploration Rover mission, J. Geophys. Res. 108 (2003) 8082, http://dx.doi.org/10.1029/2002JE002022.
[96] A.S. McEwen, M.C. Malin, M.H. Carr, W.K. Hartmann, Voluminous volcanism on early Mars revealed in Valles Marineris, Nature 397 (1999) 584–586.
[97] R.A. Duraiswami, T.N. Shaikh, Geology of the saucer-shaped sill near Mahad, western Deccan Traps, India, and its significance to the flood basalt model, Bull. Volcanol. 75 (2013) 731, http://dx.doi.org/10.1007/s00445-013-0731-4.
[98] S. Self, T. Thordarson, L. Keszthelyi, G.P.L. Walker, K. Hon, M. T. Murphy, P. Long, S. Finnermore, A new model for the emplacement of Columbia River basalts as large, inflated pahoehoe lava flow fields, Geophys. Res. Lett. 23 (1996) 2689–2692.
[99] C. Vye-Brown, S. Self, T.L. Barry, Architecture and emplacement of flood basalt flow fields: case studies from the Columbia River Basalt Group, NW USA, Bull. Volcanol. 75 (2013) 697, http://dx.doi.org/10.1007/s00445-013-0697-2.
[100] D. Mège, P. Masson, A plume tectonics model for the Tharsis province, Mars. Planet. Space Sci. 44 (1996) 1499–1546.
[101] B. Langlais, V. Lesur, M.E. Purucker, J.E.P. Connerney, M. Mandea, Crustal magnetic fields of terrestrial planets, Space Sci. Rev. 152 (2010) 223–249, http://dx.doi.org/10.1007/s11214-009-9557-y.
[102] L. Le Deit, O. Bourgeois, D. Mège, E. Hauber, S. Le Mouélic, M. Massé, R. Jaumann, J.-P. Bibring, Morphology, stratigraphy, and mineralogical composition of a layered formation covering the plateaus around Valles Marineris, Mars: implications for its geological history, Icarus, 208, , 2010, 684–703.
[103] B.M. Hynek, S.J. Robbins, O. Šrámek, S.J. Zhong, Geological evidence for a migrating Tharsis plume on early Mars, Earth Planet. Sci. Lett. 310 (2011) 327–333, http://dx.doi.org/10.1016/j.epsl.2011.08.020.
[104] S. Zhong, Migration of Tharsis volcanism on Mars caused by differential rotation of the lithosphere, Nat. Geosci. 2 (2009) 19–23, http://dx.doi.org/10.1038/ngeo392.
[105] J.-P. Williams, D.A. Paige, C. Manning, Layering in the wall rock of Valles Marineris: intrusive and extrusive magmatism, Geophys. Res. Lett. 30 (2003) 1623, http://dx.doi.org/10.1029/2003GL017662.
[106] D. Mège, P. Masson, Amounts of stretching in Valles Marineris, Mars, Planet. Space Sci. 44 (1996) 749–1582.
[107] R.A. Schultz, Structural development of Coprates Chasma and wester Ophir Planum, Valles Marineris rift, Mars, J. Geophys. Res. 96 (1991) 22,777–22,792.
[108] R.A. Schultz, Gradients in extension and strain at Valles Marineris, Mars. Planet. Space Sci. 43 (1995) 1561–1566.
[109] P.M. Grindrod, N.H. Warner, Erosion rate and previous extent of interior lauered deposits on Mars revelead by obstructed landslides, Geology 42 (2014) 795–798, http://dx.doi.org/10.1130/G35790.1.
[110] J. Michalski, P.B. Niles, Atmospheric origin of Martian intereior layered deposits: links to climte change and the global sulfur cycle, Geology 40 (2012) 419–422, http://dx.doi.org/10.1130/G32971.1.
[111] E.S. Kite, I. Halevy, M. Kahre, M.J. Wolff, M. Manga, Seasonal melting and the formation of sedimentary rocks on Mars, with predictions for the Gale Crater mound, Icarus 223 (2013) 181–210, http://dx.doi.org/10.1016/j.icarus.2012.11.034.
[112] M. Massé, M. Le Mouélic, O. Bourgeois, J.-P. Combe, L. Le Deit, C. Sotin,, J.-P. Bibring, B. Gondet, Y. Langevin, Mineralogical composition, structure, morphology, and geological history of Aram Chaos crater fill on Mars derived from OMEGA Mars Express data, J. Geophys. Res. 113, E12006, 10.1029/2008JE003131.
[113] M. Gourronc, O. Bourgeois, D. Mège, S. Pochat, B. Bultel, M. Massé, L. Le Deit, S. Le Mouélic, D. Mercier, One million cubic kilometers of fossil ice in Valles Marineris: relicts of a 3.5?Gy old glacial landsystem along the Martian equator, Geomorphology 204 (2014) 235–255, http://dx.doi.org/10.1016/j.geomorph.2013.08.009.
[114] A.S. McEwen, L. Ojha, C.M. Dundas, S.S. Mattson, S. Byrne, J.J. Wray, S.C. Cull, S.L. Murchie, N. Thomas, V.C. Gulick, Seasonal flows on warm Martian slopes, Science 333 (2011) 740–743.
[115] A.S. McEwen, C.M. Dundas, S.S. Mattson, A.D. Toigo, L. Ojha, J. J. Wray, M. Chojnacki, S. Byrne, S.L. Murchie, N. Thomas, Recurring slope lineae in equatorial regions of Mars, Nat. Geosci. 7 (2013) 53–58, http://dx.doi.org/10.1038/NGEO2014.
[116] L. Ohja, A. McEwen, C. Dundas, C. Byrne, S. Mattson, J. Wray, M. Massé, E. Schaeffer, HiRISE observations or recurring slope lineae (RSL) during southern summer on Mars, Icarus 231 (2014) 365–376, http://dx.doi.org/10.1016/j.icarus.2013.12.021.
[117] L. Ojha, M.B. Wilhelm, S.L. Murchie, A.S. McEwen, J.J. Wray, J. Hanley, M. Massé, M. Chojnacki, Spectral evidence for hydrated

salts in recurring slope lineae on Mars, Nat. Geosci. 8 (2014) 829–832, http://dx.doi.org/10.1038/NGEO2546.
[118] J. Flahaut, C. Quantin, H. Clnet, P. Allemand, J.F. Mustard, P. Thomas, Pristine Noachian crust and key geologic transitions in the lower walls of Valles Marineris: insights into early igneous processes on Mars, Icarus 221 (2012) 420–435, http://dx.doi.org/10.1016/j.icarus.2011.12.027.
[119] D. Mège, O. Bourgeois, Equatorial glaciations on Mars revealed by gravitational collapse of Valles Marineris wallslopes, Earth Planet. Sci. Lett. 310 (2011) 182–191, http://dx.doi.org/10.1016/j.epsl.2011.08.030.
[120] L. Le Deit, E. Hauber, F. Fueten, M. Pondrelli, A.P. Rossi, R. Jaumann, Sequence of infilling events in Gale Crater, Mars: results from morphology, stratigraphy, and mineralogy, J. Geophys. Res., 118, , 2013, 1–35, http://dx.doi.org/10.1002/2012JE004322.
[121] M.T. Brunetti, F. Guzzetti, M. Cardinali, F. Fiorucci, M. Santangelo, P. Mancinelli, G. Komatsu, L. Borselli, Analysis of a new geomorphological inventory of landslides in Valles Marineris, Mars, Earth Planet. Sci. Lett. 05 (2014) 156–168.
[122] C. Huggel, S. Zgraggen-Oswald, W. Haeberli, A. Kääb, A. Polkvoj, I. Galushkin, S.G. Evans, The 2002 rock/ice avalanche at Kolka/Karmadon, Russian Caucasus: assessment of extraordinary avalanche formation and mobility, and application of QuickBird satellite imagery, Nat. Hazards Earth Syst. Sci. 5 (2005) 173–187.
[123] I. Baron, M. Kernstocková, M. Faridi, M. Bubík, R. Milovský, R. Melichar, J. Sabouri, J. Baburek, Paleostress analysis of a gigantic gravitational mass movement in active tectonic setting: the Qoshadagh slope failure, Ahar, NW Iran, Tectonophysics 605 (2013) 70–87.
[124] J. Flahaut, J. Mustard, C. Quantin, H. Clenet, P. Allemand, P. Thomas, Dikes of distinct composition intruded into Noachian-aged crust exposed in the walls of Valles Marineris, Geophys. Res. Lett. 38 (2011) L15202, http://dx.doi.org/10.1029/2011GL048109.
[125] E.M. Anderson, The Dynamics of Faulting and Dyke Formation With Applications to Britain, Oliver & Boyd, Edinburgh, 1951.
[126] O.H. Muller, D.D. Pollard, The stress state near Spanish Peaks, Colorado determined from a dike pattern, Pure Appl. Geophys. 115 (1977) 69–86.
[127] A. Spiga, F. Forget, A new model to simulate the Martian mesoscale and microscale atmospheric circulation: validation and first results, J. Geophys. Res. 114 (2009) E02009, http://dx.doi.org/10.1029/2008JE003242.
[128] G. Baer, Mechanisms if dike propagation in layered rocks and massive, porous sedimentary rocks, J. Geophys. Res. 96 (B7) (1991) 11911–11929.
[129] J.-P. Callot, L. Geoffroy, C. Aubourg, J.-P. Pozzi, D. Mège, Magma flow directions of shallow dykes from the East Greenland volcanic margin inferred from magnetic fabric studies, Tectonophysics 335 (2001) 313–329.
[130] R.A. Schultz, D. Mège, H. Diot, Emplacement conditions of igneous dikes in the Ethiopian Traps, J. Volcanol. Geotherm. Res. 178 (2008) 683–692, http://dx.doi.org/10.1016/j.jvolgeores.2008.08.012.
[131] H.L. Petcovic, A.L. Grunder, Textural and thermal history of partial melting in tonalitic wallrock at the margin of a basalt dike, Wallowa Mountains, Oregon, J. Petrol. 44 (2003) 2287–2312, http://dx.doi.org/10.1093/petrology/egg078.
[132] H.L. Petcovic, J.D. Dufek, Modeling magma flow and cooling in dikes: implications for emplacement of Columbia River flood basalts, J. Geophys. Res. 110 (2005) B10201, http://dx.doi.org/10.1029/2004JB003432.
[133] I.M. Platten, Incremental dilation of magma filled fractures: evidence from dykes on the Isle of Skye, Scotland, J. Struct. Geol. 22 (2000) 1153–1164.
[134] A.S. McEwen, M.S. Robinson, E.M. Eliason, P.G. Lucey, T.C. Duxbury, P.D. Spudis, Clementine observations of the Aristarchus region of the Moon, Science 266 (1994) 1858–1861, http://dx.doi.org/10.1126/science.266.5192.1858.
[135] M. Ohtake, 31 coauthors, The global distribution of pure anorthosite on the Moon, Nature 461 (2009) 236–3241, http://dx.doi.org/10.1038/nature08317.
[136] C.M. Pieters, S. Muchie, N. Thomas, D. Britt, Composition of surface materials on the moons of Mars, Planet. Space Sci. 102 (2014) 144–151, http://dx.doi.org/10.1016/j.pss.2014.02.008.
[137] S. Chevrel, P.C. Pinet, Y. Daydou, S. Le Mouélic, Y. Langevin, F. Costard, S. Erard, The Aristarchus Plateau on the Moon: mineralogical and structural study from integrated Clementine UV-Vis-NIR spectral data, Icarus 199 (2009) 9-24.
[138] P. Chauhan, P. Kaur, N. Srivastava, S. Bhattacharya, Ajai, A.S. Kiran Kumar, J.N. Goswami, Compositional and morphological analysis of high resolution remote sensing data over central peak of Tycho crater on the Moon: implications for understanding lunar interior, Current Sci. 102 (2012) 1041-1046.
[139] B.P. Weiss, S.M. Tikoo, The lunar dynamo, Science http://dx.doi.org/10.1126/science.1246753.
[140] N. Thomas, R. Stelter, A. Ivanov, N.T. Bridges, K.E. Herkenhoff, A. S. McEwen, Spectral heterogenity on Phobos and Deimos: HiRISE observations and comparisons to Mars Pathfinder results, Planet. Space Sci. 59 (2011) 1281–1292, http://dx.doi.org/10.1016/j.pss.2010.04.018.
[141] A.T. Basilevsky, C.A. Lorenz, T.V. Shingareva, J.W. Head, K. R. Ramsley, A.E. Zubarev, The surface geology and geomorphology of Phobos, Planet. Space Sci. 102 (2014) 95–118, http://dx.doi.org/10.1016/j.pss.2014.04.013.
[142] O. Witasse, 41 coauthors, Mars Express investigations of Phobos and Deimos, Planet. Space Sci. 102 (2014) 18–34, http://dx.doi.org/10.1016/j.pss.2013.08.002.
[143] A.A. Fraeman, S.L. Murchie, R.E. Arvidson, R.N. Clark, R.V. Morris, A. S. Rivkin, F. Vilas, Spectral absorptions on Phobos and Deimos in the visible/near infrared wavelengths and their compositional constraints, Icarus 229 (2014) 196–205, http://dx.doi.org/10.1016/j.icarus.2013.11.02.
[144] T.P. Andert, P. Rosenblatt, M. Pätzold, B. Häusler, V. Dehant, G. L. Tyler, J.C. Marty, Precise mass determination and the nature of Phobos, Geophys. Res. Lett. 37 (2010) L09202, http://dx.doi.org/10.1029/2009GL041829.
[145] P. Rosenblatt, S. Charnoz, On the formation of the Martian moons from a circum-martian accretion disk, Icarus 221 (2012) 806–815, http://dx.doi.org/10.1016/j.icarus.2012.09.009.
[146] S.L. Murchie, T. Britt, C.M. Pieters, The value of Phobos sample return, Planet. Space Sci. 102 (2014) 176–182, http://dx.doi.org/10.1016/j.pss.2014.04.014.
[147] M. Pätzold, M. Andert, R. Jacobson, P. Rosenblatt, V. Dehant, Phobos: observed bulk properties, Planet. Space Sci. (2014) 86–94.
[148] P. Rosenblatt, The origin of the Martian moons revisited, Astron. Astrophys. Rev. 19 (2011) 44, http://dx.doi.org/10.1007/s00159-011-0044-6.
[149] J. Oberst, A. Zubarev, I. Nadezhdina, L. Shishkina, N. Rambaux, The Phobos geodetic control point network and rotation model, Planet. Space Sci. 102 (2014) 45–50, http://dx.doi.org/10.1016/j.pss.2014.03.006.
[150] A.R. Dobrovolskis, Internal stresses in Phobos and other triaxial bodies, Icarus 52 (1982) 136–148.
[151] S. Le Maistre, P. Rosenblatt, N. Rambaux, J.C. Castillo-Rogez, V. Dehant, J.-C. Marty, Phobos interior from librations determination using Doppler and star tracker measurements, Planet. Space Sci. 85 (2013) 106–122, http://dx.doi.org/10.1016/j.pss.2013.06.015.
[152] M. Efroimsky, V. Lainey, Physics of bodily tides in terrestrial planets and the appropriate scales of dynamical evolution, J. Geophys. Res. 112 (2007) E12003, http://dx.doi.org/10.1029/2007JE002908.
[153] P. Rosenblatt, The origin of the Martian moons revisited, in: Proceedings of the 46th ESLAB Symposium: Formation and evolution of moons, ESTEC, Noordwijk, the Netherlands, Abstract, 2012.
[154] I. Sharma, The equilibrium of rubble-pile satellites: the Darwin and Roche ellipsoids for gravitationally held granular aggregates, Icarus 200 (2009) 636-654.
[155] A. Zakharov, M. Horanyi, P. Lee, O. Witasse, F. Ciprinai, Dust at the Martian moons and in the circummartian space, Planet. Space Sci. 102 (2014) 171–175, http://dx.doi.org/10.1016/j.pss.2013.12.011.
[156] T.A. Przylibski, K. Luszczek, Mineral resources of extraterrestrial bodies of the Solar System, Mineral. Spec. Pap. 40 (2012) 51–52.
[157] M. Elvis, How many ore-bearing asteroids? Planet. Space Sci. 91 (2014) 20–26.
[158] R.P. Binzel, S.J. Bus, S. Xu, J. Sunshine, T.H. Burbine, Rotationally resolved spectra of asteroid 16 Psyche, Icarus 117 (1995) 443–445.
[159] A. Dollfus, M. Duseaux, J.C. Mandeville, Are some asteroids pieces of metal? in: Proceedings of the 8th Lunar Science Conference, 1977, pp.?242 244.
[160] D.R. Davis, P. Farinella, F. Marzari, The missing Psyche family: collisionally eroded or never formed? Icarus 137 (1999) 140–151.
[161] A. Dollfus, J.C. Mandeville, M. Duseaux, The nature of the M-Type asteroids from optical polarimetry, Icarus 37 (1979) 124–132.
[162] M. Elvis, Let's mine asteroids – for science and profit, Nature 485 (2012) 549.